An NAC Transcription Factor Controls Ethylene-Regulated Cell Expansion in Flower Petals[1][C][W][OPEN]

Haixia Pei, Nan Ma, Ji Tian, Jing Luo, Jiwei Chen, Jing Li, Yi Zheng, Xiang Chen, Zhangjun Fei, and Junping Gao*

Department of Ornamental Horticulture, China Agricultural University, Beijing 100193, China (H.P., N.M., J.T., J.Lu., J.C., J.Li, Y.Z., X.C., J.G.); Boyce Thompson Institute for Plant Research, Cornell University, Ithaca, New York 14853 (Y.Z., Z.F.); and United States Department of Agriculture Robert W. Holley Center for Agriculture and Health, Ithaca, New York 14853 (Z.F.)

ORCID ID: 0000-0002-9285-2539 (J.G.).

Cell expansion is crucial for plant growth. It is well known that the phytohormone ethylene functions in plant development as a key modulator of cell expansion. However, the role of ethylene in the regulation of this process remains unclear. In this study, 2,189 ethylene-responsive transcripts were identified in rose (*Rosa hybrida*) petals using transcriptome sequencing and microarray analysis. Among these transcripts, an NAC (for no apical meristem [NAM], Arabidopsis transcription activation factor [ATAF], and cup-shaped cotyledon [CUC])-domain transcription factor gene, *RhNAC100*, was rapidly and dramatically induced by ethylene in the petals. Interestingly, accumulation of the *RhNAC100* transcript was modulated by ethylene via *microRNA164*-dependent posttranscriptional regulation. Overexpression of *RhNAC100* in Arabidopsis (*Arabidopsis thaliana*) substantially reduced the petal size by repressing petal cell expansion. By contrast, silencing of *RhNAC100* in rose petals using virus-induced gene silencing significantly increased petal size and promoted cell expansion in the petal abaxial subepidermis ($P < 0.05$). Expression analysis showed that 22 out of the 29 cell expansion-related genes tested exhibited changes in expression in *RhNAC100*-silenced rose petals. Moreover, of those genes, one cellulose synthase and two aquaporin genes (*Rosa hybrida Cellulose Synthase2* and *R. hybrida Plasma Membrane Intrinsic Protein1;1/2;1*) were identified as targets of RhNAC100. Our results suggest that ethylene regulates cell expansion by fine-tuning the *microRNA164/RhNAC100* module and also provide new insights into the function of NAC transcription factors.

Rose (*Rosa hybrida*) is one of the most important ornamental plants worldwide, and it has been cultivated since 500 BC. The morphological changes occurring during flower opening typically consist of petal outgrowth and unfurling, processes that are also important horticulturally for rose flowers. Petal growth is a complex process that integrates cell division and cell expansion. In Arabidopsis (*Arabidopsis thaliana*), cell division is typically phased out in petals prior to bud opening and flower development, and cell expansion predominantly contributes to petal growth at later stages (Irish, 2008). Similarly, in rose, petal growth also largely depends upon cell expansion at later stages of flower opening (Yamada et al., 2009).

Ethylene, an important plant hormone, regulates various plant developmental processes including seed germination, organ elongation, flowering, fruit ripening, organ senescence, and abscission (Abeles et al., 1992). Although several reports have demonstrated that ethylene stimulates cell division (Ortega-Martinez et al., 2007; Love et al., 2009), it typically functions in plant development as a key modulator of cell expansion. In Arabidopsis, dark-grown seedlings treated with ethylene exhibit a triple response, which consists of radial swelling of the hypocotyl, exaggeration of the apical hook, and inhibition of hypocotyl and root elongation (Guzmán and Ecker, 1990). The constitutive ethylene-responsive mutant *constitutive triple response1* (*ctr1*) shows severe dwarfism and much smaller leaf cell sizes compared with wild-type plants (Kieber et al., 1993). It has been reported that ethylene can inhibit elongation of leaves in *Poa* species and roots in *Rumex palustris* and *Cucumis sativus* (Pierik et al., 2006). In rose, we previously showed that ethylene accelerates the flower-opening process but inhibits the expansion of petal abaxial subepidermis (AbsE) cells, thereby further inhibiting petal expansion (Ma et al., 2008). To date, the ethylene-responsive regulatory mechanism that arises during cell expansion remains unclear, although several reports have demonstrated that ethylene regulates the expression of genes associated with cell expansion, such as cell wall metabolism

[1] This work was supported by the National Natural Science Foundation of China (grant nos. 31130048 and 30671480 to J.G.).

* Address correspondence to gaojp@cau.edu.cn.

The author responsible for distribution of materials integral to the findings presented in this article in accordance with the policy described in the Instructions for Authors (www.plantphysiol.org) is: Junping Gao (gaojp@cau.edu.cn).

[C] Some figures in this article are displayed in color online but in black and white in the print edition.

[W] The online version of this article contains Web-only data.

[OPEN] Articles can be viewed online without a subscription.

www.plantphysiol.org/cgi/doi/10.1104/pp.113.223388

and transporter genes (Zhong and Burns, 2003; De Paepe et al., 2004; Alba et al., 2005).

As regulators of gene expression, transcription factors (TFs) play an important role in plant development and in the response to hormone signals (Riechmann et al., 2000). NAC (for no apical meristem [NAM], Arabidopsis transcription activation factor [ATAF], and cup-shaped cotyledon [CUC])-domain proteins comprise one of the largest families of plant-specific TFs. Many NAC-domain genes have been identified from a range of plant species, including Arabidopsis (Riechmann et al., 2000), rice (*Oryza sativa*; Xiong et al., 2005), tobacco (*Nicotiana tabacum*; Rushton et al., 2008), poplar (*Populus* spp.; Hu et al., 2010), and soybean (*Glycine max*; Pinheiro et al., 2009). The NAC superfamily can be divided into at least seven subfamilies (Rushton et al., 2008), and the function of NAC genes is typically subfamily specific. In Arabidopsis, members of the NAM subfamily *CUC1/CUC2/CUC3* are well known as regulators involved in shoot apical meristem formation and cotyledon separation during embryogenesis (Aida et al., 1997; Olsen et al., 2005), whereas members of the Vascular-related NAC-Domain protein/NAC Secondary wall Thickening promoting factor/Secondary wall-associated NAC-Domain protein (*VND/NST/SND1*) subfamily are typically involved in regulating secondary wall formation (Yamaguchi and Demura, 2010). Previous reports have indicated that several *NAC* genes may be regulated by ethylene. In a tomato (*Solanum lycopersicum*) plant, at least one *NAC* gene is influenced by the mutation of *Never Ripe*, which is a gene encoding an ethylene receptor (Alba et al., 2005). In Arabidopsis, mutation of *ETHYLENE INSENSITIVE2* (*EIN2*) blocked the induction of *Arabidopsis NAC092* (*ANAC092*)/*AtNAC2*/*ORESARA1* (*ORE1*) expression under salt conditions (He et al., 2005). Microarray analysis has revealed that approximately one-third of *NAC* genes are regulated by application of 1-aminocyclopropane-1-carboxylate, which is a precursor of ethylene, in Arabidopsis (Jensen et al., 2010). In addition to transcriptional regulation, several *NAC* genes, including *NAC1* and a few members of the NAM subfamily are also posttranscriptionally regulated by *microRNA164* (*miR164*; Sieber et al., 2007). Auxin can increase the abundance of *miR164* and thus decrease transcript accumulation of *NAC1*, which is a target of *miR164*, thereby promoting lateral root initiation in Arabidopsis (Guo et al., 2005). Increased *miR164* levels have also been reported in *ein2-1*, which is an ethylene-insensitive mutant. However, the question of whether NAC genes are involved in ethylene-regulated floral organ growth remains unclear.

In this study, potential key regulators that mediate ethylene-regulated cell expansion in rose petals were screened using microarray analysis. One hundredfive ethylene-responsive TFs and regulators were identified from rose petals. *RhNAC100*, a homolog of *ANAC092*/*AtNAC2*/*ORE1* in Arabidopsis, was found to function as a negative regulator of cell expansion in petals. Accumulation of *RhNAC100* transcripts is regulated by *miR164* in vivo in an ethylene-dependent manner, and RhNAC100 is capable of binding to promoters of the cell expansion-related genes *R. hybrida Cellulose Synthase2* (*RhCesA2*) and *R. hybrida Plasma Membrane Intrinsic Protein1;1/2;1* (*RhPIP1;1/RhPIP2;1*). Taken together, these data reveal an ethylene-mediated *miR164/RhNAC100* module and identify a set of cell expansion-related genes that are regulated by this module during petal cell expansion in rose and transgenic Arabidopsis.

RESULTS

Transcriptome Sequencing of Rose Flowers

To investigate the molecular mechanism of ethylene-regulated flower opening, firstly, large scale transcriptome sequencing of ethylene-treated and control flowers were performed using 454 massive parallel pyrosequencing technology. (Primers for library construction are listed in Supplemental Table S1.) We obtained 60,944 assembled transcripts with an average length of 302 bp and a total length of approximately 18.4 million base pair (Mb; Supplemental Fig. S1; see Supplemental Text S1 for detailed analysis). The assembled transcript sequences were compared against National Center for Biotechnology Information nonredundant, UniProt, and the TAIR9 release of The Arabidopsis Information Resource protein databases, respectively, using blast with the e-value cutoff set to 1e–5. The results showed that 33,763 transcripts (55.4%) had significant matches in the databases. The annotated assembled transcripts were classified into different functional categories according to a set of plant-specific gene ontology (GO) slims. A total of 26,462 were assigned with at least one GO term, and 21,331, 23,868, and 19,229 were assigned with GO term in biological process, molecular function, and cellular component categories, respectively (Supplemental Table S2). All these analyses supported that the sequences generated in this study provide a valuable resource for rose gene discovery and functional analyses. The raw sequence data were deposited into the National Center for Biotechnology Information Sequence Read Archive database under accession number SRA045958, and the processed sequence reads and assembled transcript sequences are also available at the rose transcriptome database (http://bioinfo.bti.cornell.edu/rose).

Identification of Ethylene-Responsive Genes in Rose Petals Using Microarray Analysis

To investigate the molecular mechanism underlying ethylene-regulated flower opening, we first designed and constructed an oligonucleotide microarray containing probes representing 14,997 rose assembled transcripts, which were extracted from a rose floral transcriptome database (http://bioinfo.bti.cornell.edu/rose).

This custom microarray was used to investigate gene expression profiles in rose petals following ethylene treatment. A total of 2,189 assembled transcripts in petals were significantly regulated by ethylene (false discovery rate [FDR] < 0.05 and fold changes ≥ 2), and these transcripts were divided into three groups based on their expression patterns (Fig. 1A; Supplemental Table S3). Interestingly, 386 ethylene-responsive transcripts exhibited rapid responses to ethylene (within 1 h), including 90 up-regulated and 296 down-regulated transcripts. Notably, the ethylene receptor and *CTR1* were among the up-regulated genes, which is consistent with our previous report (Tan et al., 2006). Many genes involved in cell expansion-related processes, such as cell wall catabolism, water transportation, and hexose transport, were responsive to ethylene. For example, the expression of 22 out of the 26 water transporter genes on the microarray showed significant repression, including two that had been previously shown to be down-regulated following ethylene treatment (Ma et al., 2008; Xue et al., 2009). In addition, 105 ethylene-responsive transcripts were identified as TFs and transcriptional regulators (TRs), which were grouped into 23 families (Fig. 1B; Supplemental Table S4). The major families included myeloblastosis (14 transcripts), APETALA2/ethylene-responsive element-binding protein (12 transcripts), homeobox domain (11 transcripts), WRKY (10 transcripts), basic helix-loop-helix (bHLH; 10 transcripts), GIBBERELLIC-ACID INSENSITIVE, REPRESSOR OF GA1-3 SCARECROW (10 transcripts), and NAC-domain family (eight transcripts). Interestingly, 14 TFs and TRs were involved in the signaling cascades of auxin (two auxin response factors [ARFs] and four Auxin/Indole-3-acetic acid [AUX/IAA] inducible genes), gibberellin (five DELLAs), or brassinosteroid (three BR Enhanced Expressions [BEEs]).

RhNAC100 Encodes an Ethylene-Inducible NAC-Domain TF

To identify potential key regulators involved in ethylene-regulated petal expansion in rose, we focused primarily on an analysis of expression profiles of TFs

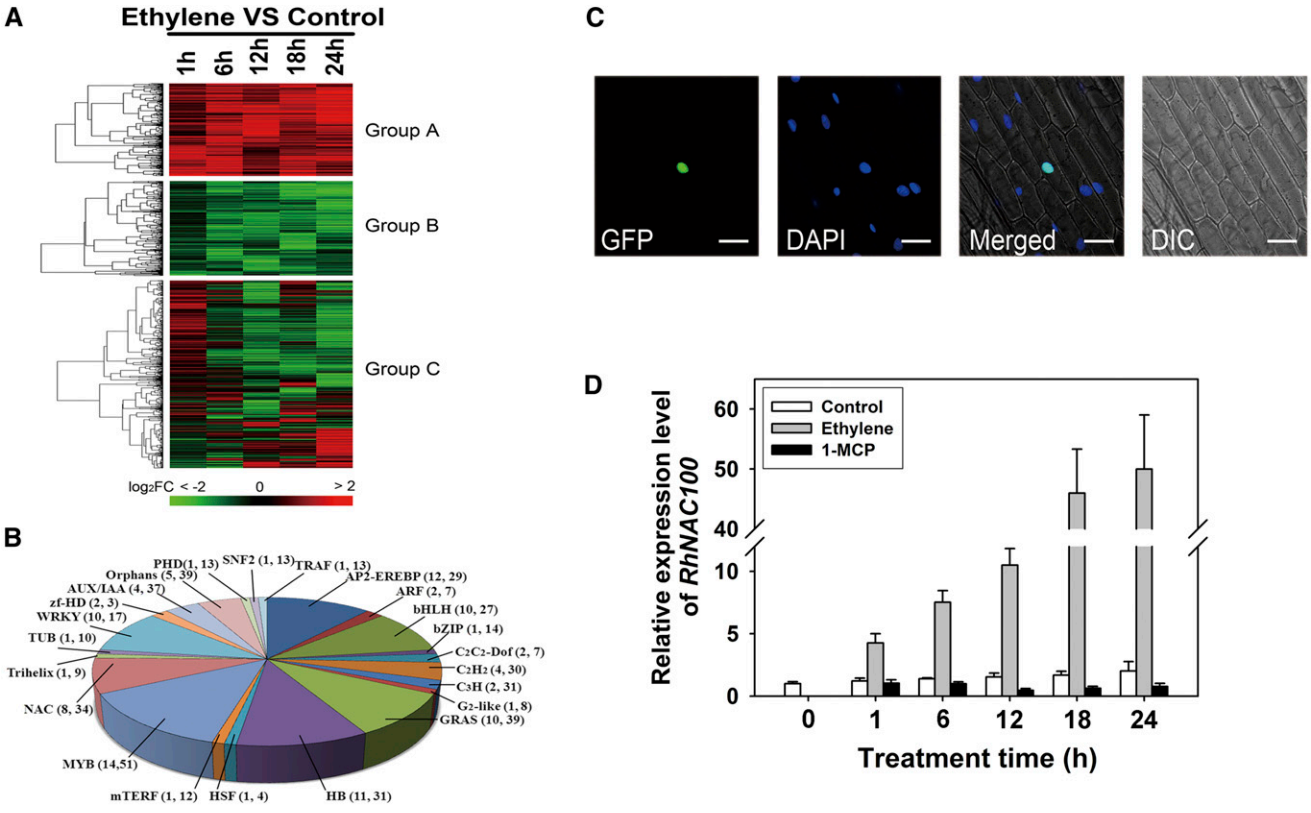

Figure 1. Screening of ethylene-responsive genes in rose petals and characterization of *RhNAC100*. A, Expression profiles of genes following ethylene treatment of rose petals. Log-of-fold changes in each probe set responding to ethylene at 1-, 6-, 12-, 18-, and 24-h ethylene treatment were used to generate the cluster. B, Ethylene-responsive TFs and TRs. The numbers in the parentheses after each TF or TR family indicate the number of changed TFs or TRs (first number) and the number of tested TFs or TRs on the microarray (second number). C, Subcellular localization of RhNAC100 in onion epidermal cells. Bar = 100 μm. D, qRT-PCR analysis of *RhNAC100* in response to ethylene in petals. The results show the mean $\pm$ SD (error bars) of qRT-PCR experiments and were generated from three biological replicates, each with three technical replicates. *RhACT5* was used as the internal control.

and TRs in response to ethylene. The expression of RU02822, a putative NAC-domain TF, was rapidly and robustly induced by ethylene (Supplemental Table S4). The coding region of RU02822 contains 1,020 nucleotides, and it encodes a putative protein containing 339 amino acids. Sequence analysis indicated that RU02822 contains a typical NAC-domain consisting of five conserved amino acid motifs (N1–N5; Olsen et al., 2005) in its N terminus, whereas its C-terminal domain is quite specific (Supplemental Fig. S2A). *RU02822* was named as *RhNAC*100 (JQ001774) because its closest homolog is *ANAC100* in Arabidopsis. Phylogenetic analysis indicated that RhNAC100 belongs to the NAM subfamily of the NAC-domain TF family (Supplemental Fig. S2B), which has been reported to be involved in cotyledon, leaf, and petal development in Arabidopsis (Laufs et al., 2004; Baker et al., 2005; Kim et al., 2009; Hasson et al., 2011). Quantitative reverse transcription (qRT)-PCR showed that expression of *RhNAC100* was detected in petals, leaves, and roots of rose (Supplemental Fig. S2C).

Interestingly, N terminus of RhNAC100 also contains an NARD (NAC repression domain) domain (Supplemental Fig. S2A), which was recently reported to be a conserved and active repression domain in NAC proteins (Hao et al., 2010), suggesting that RhNAC100 may function as a transcription repressor. In addition, we performed transactivation analyses in leaf protoplast of Arabidopsis using VP16 (viral protein16 from herpes simplex) transcriptional activation domain as the positive control (Hao et al., 2010). The results showed that RhNAC100 could clearly repress the transcription activity of VP16, implying that RhNAC100 could function as a repressor (Supplemental Fig. S2D).

A transient expression assay in onion (*Allium cepa*) epidermal cells showed that RhNAC100-Enhanced GFP fusion protein is localized to the nucleus, thereby supporting the theory that RhNAC100 is a TF (Fig. 1C). qRT-PCR showed that the expression of *RhNAC100* rapidly and dramatically increased by approximately 6-fold following ethylene treatment (1 h) and was clearly inhibited following 1-methylcyclopropene (1-MCP) treatment. 1-MCP is a strong inhibitor of ethylene function that is capable of binding to the ethylene receptor and preventing the physiological action of ethylene (Sisler and Serek, 1997). These results confirmed our microarray analysis (Fig. 1D). In addition, *RhNAC100* expression was suppressed by auxin and GA treatments, whereas it was not altered following treatment with brassinosteroid (Supplemental Fig. S3).

Ethylene Fine-Tunes the Accumulation of *RhNAC100* Transcripts by Repressing *miR164*

To understand how ethylene regulates *RhNAC100* expression, we first isolated the promoter of *RhNAC100* and analyzed the sequence using the PLACE database (http://www.dna.affrc.go.jp/PLACE/). Unexpectedly, no ethylene-responsive elements were found (Supplemental Fig. S4A). In Arabidopsis, three members of the NAM subfamily, *ANAC092/AtNAC2/ORE1* (*AT5G39610*), *CUC1* (*AT3G15170*), and *ANAC100* (*AT5G61430*), are ethylene-inducible, although they do not contain any ethylene-responsive elements in their promoter regions (Jensen et al., 2010). However, all of these genes are targets of *miR164*, a conserved family of plant microRNAs (miRNAs; Sieber et al., 2007). Here, we also found that *RhNAC100* possesses a potential *miR164* binding site located in the third exon (Fig. 2A). This *miR164* cleavage site was verified using modified RNA ligase-mediated 5′-RACE, and sequencing analysis revealed that six out of the 10 independent complementary DNA (cDNA) clones were cleaved at the position between the tenth and eleventh nucleotide from the 5′ end of *miR164* (Fig. 2A), which is identical to the cleavage position noted in Arabidopsis (Mallory et al., 2004; Guo et al., 2005; Nikovics et al., 2006; Sieber et al., 2007; Kim et al., 2009). These results indicate that *RhNAC100* is a potential target of *miR164* in rose.

To verify whether the accumulation of *RhNAC100* transcripts is posttranscriptionally regulated by *miR164*, *miR164* was obtained from rose petals and named *rhy-miR164*. The sequence of *rhy-miR164* was identical to the *miR164* sequence in Arabidopsis (Fig. 2A) and was consistent with a recent report in rose (Kim et al., 2012). The *rhy-miR164* abundance in ethylene-treated rose petals was reduced to 48.8% of that of control petals. Conversely, 1-MCP treatment increased the abundance of *rhy-miR164* in rose petals (Fig. 2B). The abundance of *RhNAC100* transcripts in rose petals was substantially increased following ethylene treatment and the expression pattern of *RhNAC100* was inversely correlated to that of *rhy-miR164* (Figs. 1D and 2B).

To test whether the ethylene-induced accumulation of *RhNAC100* transcripts resulted from the decreased level of *rhy-miR164* in rose petals, we generated *RhNAC100m*, an *miR164*-resistant version of *RhNAC100*, by substituting six nucleotides in the *miR164/RhNAC100* complementary region to produce mismatches without changing the amino acid sequence (Fig. 2A). *MiR164* is a well-conserved miRNA in plants, and the mature sequence of *rhy-miR164* is identical to *miR164* in Arabidopsis. According to the principles of target reorganization and cleavage by miRNA (Bartel, 2009), *RhNAC100* could be targeted and cleaved properly in Arabidopsis. Thus, we generated transgenic Arabidopsis overexpressing *RhNAC100* and *RhNAC100m* (an *miR164*-resistant version of *RhNAC100*) in wild-type Arabidopsis (ecotype Columbia [Col-0]) and in *ein2-1* mutant to evaluate the cleaving activity of Arabidopsis *miR164* on rose *RhNAC100* with and without ethylene.

In plants, miRNA-guided cleavage of target mRNAs produces both the 5′ and 3′ cleavage fragments. Although both 5′ and 3′ cleavage fragments are degraded, in many instances, the 3′ cleavage fragment is

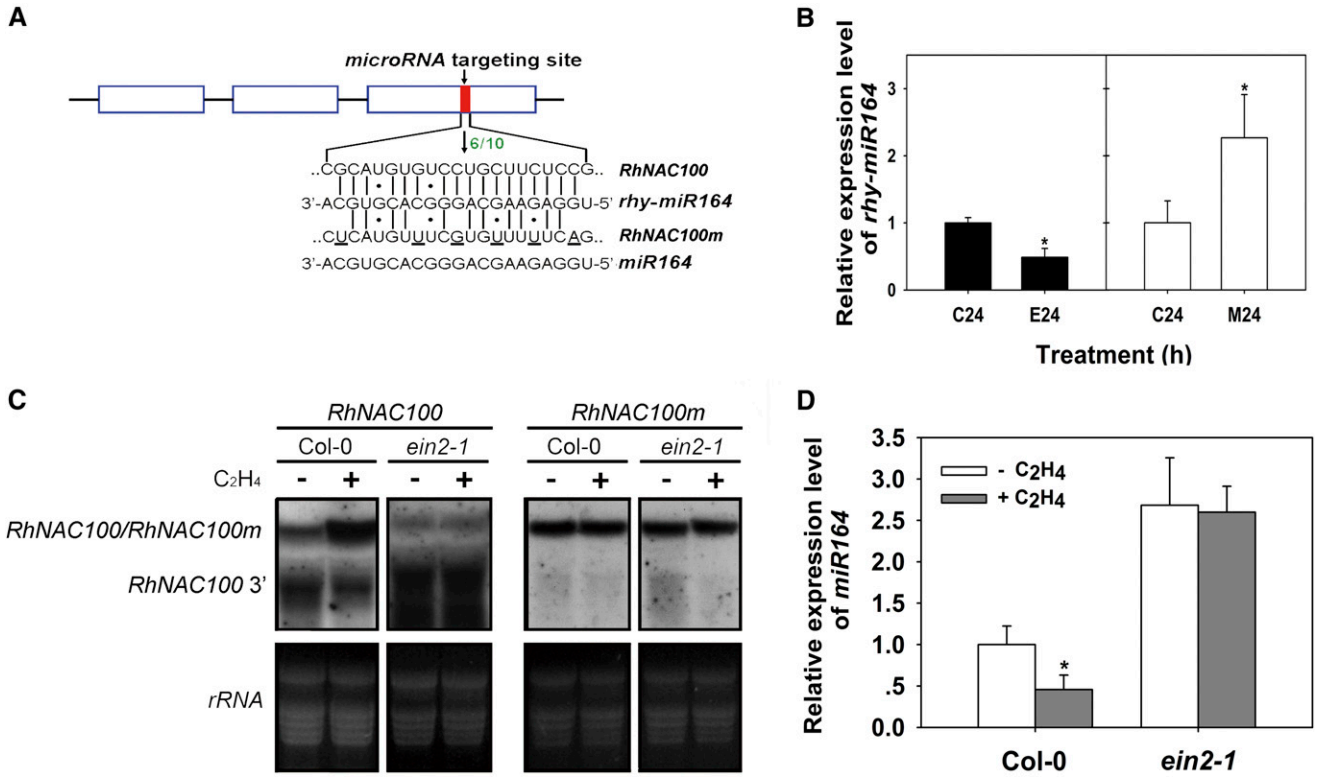

Figure 2. Cleavage of *RhNAC100* mRNA by *miR164*. A, A schematic representation of *RhNAC100* and alignment of *rhy-miR164* with *RhNAC100* (normal) and *RhNAC100* mutated (*RhNAC100m*) transcripts. Short vertical lines represent Watson-Crick pairing, and circles indicate G:U wobble pairing. The vertical arrow indicates the 5′ termini of miRNA-guided cleavage products, and the frequencies of the clones are also shown. The mutant nucleotides are underlined. *rhy-miR164* and *ath-miR164* are *miR164* sequences in rose and Arabidopsis, respectively. B, qRT-PCR of *rhy-miR164* in rose petals. Flowers (stage 2) were exposed to air (–) or 10 μL L^{-1} ethylene (+) for 24 h (left). Flowers (stage 2) were exposed to air (C24), 10 μL L^{-1} ethylene (E24), or 2 μL L^{-1} 1-MCP (M24) for 24 h (right). qRT-PCR was performed on at least three biological replicates. Bars indicate the SD (Student's *t* test, $*P < 0.05$). The internal control used was 5S rRNA. C, Effect of ethylene on *miR164*-directed cleavage of *RhNAC100* in Arabidopsis. The full-length *RhNAC100* transcript and its 3′ fragments cleaved by *miR164* are indicated. *rRNA* visualized by ethidium bromide staining was used as a loading control. Six biological replicates were used, and representative results are shown. D, qRT-PCR of *ath-miR164* from Arabidopsis leaves. The qRT-PCR was performed using at least three biological replicates. The internal control used was 5S rRNA. Bars indicate the SD (Student's *t* test, $*P < 0.05$). [See online article for color version of this figure.]

more stable and thus detectable (Llave et al., 2002; Dunoyer et al., 2004; Souret et al., 2004). In *RhNAC100*-ox/Col transgenic plants, both the full-length transcript and the 3′ cleavage fragment of *RhNAC100* were detected. Ethylene treatment dramatically increased the levels of full-length *RhNAC100* transcript, whereas it decreased the levels of the *RhNAC100* 3′ cleavage fragment in *RhNAC100*-ox/Col plants. By contrast, the amount of the full-length *RhNAC100* was lower and that of the cleaved 3′ fragment was higher in *RhNAC100*-ox/*ein2* plants, indicating that the cleavage of *RhNAC100* was enhanced in the *ein2-1* mutant. In addition, ethylene treatment was unable to change the abundance of either intact transcripts or 3′ cleavage fragments of *RhNAC100* in *RhNAC100*-ox/*ein2* plants. In both *RhNAC100m*-ox/Col and *RhNAC100m*-ox/*ein2* transgenic plants, full-length *RhNAC100* transcripts were highly accumulated, whereas the 3′ cleavage fragment was undetectable. Moreover, the abundance of intact *RhNAC100m* transcripts was almost identical in *RhNAC100m*-ox/Col and *RhNAC100m*-ox/*ein2* plants with or without ethylene treatment (Fig. 2C), indicating that ethylene-regulated accumulation of the *RhNAC100* transcript was mediated via a suppression of *miR164*-guided cleavage of *RhNAC100*. Consistent with a previous report (Kim et al., 2009), levels of *miR164* were greater in the *ein2-1* mutant than in the Col-0 control plants. Furthermore, levels of *miR164* decreased following ethylene treatment in the Col-0 plants, whereas the level was not influenced by ethylene in the *ein2-1* mutants (Fig. 2D). On the basis of these results, it was hypothesized that ethylene could fine-tune the accumulation of *RhNAC100* transcripts by repressing *miR164* and that this regulatory process requires *EIN2*. To test this hypothesis during the natural opening process of rose flowers, we determined

the petal AbsE cell density, ethylene production, rhy-miR164 abundance, and RhNAC100 expression in rose petals. In rose flowers, stages 0, 2, and 4 represent unopened buds, completely opened buds, and opened flowers, respectively (Ma et al., 2005). The petal AbsE cell density decreased continuously from stage 0 to 4, but the decrease was more pronounced during the earlier stages (stages 0–2) than during the later stages (stages 2–4), indicating that the petal growth rate declined as the flower opened (Fig. 3A). Petal ethylene production was relatively low during stage 0, showed a substantial increased during stage 2, and exhibited a further increase during stage 4. The abundance of *rhy-miR164* was relatively high in the petals at stage 0, whereas it decreased dramatically during stage 2 and decreased further during stage 4. By contrast, the expression of *RhNAC100* was low during stage 0 and increased substantially upon flower opening in rose petals (Fig. 3B), indicating that the expression pattern of *RhNAC100* was negatively correlated with *rhy-miR164* during flower opening. The *rhy-miR164*-directed cleavage of *RhNAC100* mRNA was monitored in rose petals during flower opening using regional amplification-PCR (Vazquez et al., 2004; Oh et al., 2008). The results demonstrated that the level of intact *RhNAC100* transcripts increased substantially upon flower opening, whereas the abundance of the *RhNAC100* 3′ fragment remained relatively stable during flower opening (Supplemental Fig. S4B), which further supports the theory that *rhy-miR164* cleaves *RhNAC100* during the natural flower-opening process.

RhNAC100 Is Involved in Cell Expansion

The phenotype of transgenic Arabidopsis plants was observed. Compared with transgenic plants expressing an empty vector, the petal size decreased by 33% to 36% in *RhNAC100*-ox/Col and by 49% to 52% in *RhNAC100m*-ox/Col plants (Fig. 4, A and B). Microscopic analysis revealed that the density of abaxial epidermal cells in the petals increased by 20% to 23% and 37% to 41% in *RhNAC100*-ox/Col and *RhNAC100m*-ox/Col plants, respectively, compared with vector/Col-0 plants ($P < 0.01$, Tukey's test; Fig. 4C). Vector/*ein2*-expressing plants produced larger petals approximately 1.4-fold) than the vector/Col-0 plants, while the abaxial epidermal cell density in the former plants was approximately 70% of the latter, indicating that blockage of the ethylene signaling pathway led to enhanced cell expansion. Compared with the vector/*ein2* line, the petal size was reduced by 21% to 22% and 49% to 57%, respectively, whereas the abaxial epidermal cell density increased by 14% to 25% and 39% to 47%, respectively, in the *RhNAC100*-ox/*ein2* and *RhNAC100m*-ox/*ein2* plants ($P < 0.01$, Tukey's test).

Because the mutation of *miR164*-binding site did not alter the deduced amino acid sequence, the function of *RhNAC100m* was supposed to be identical to

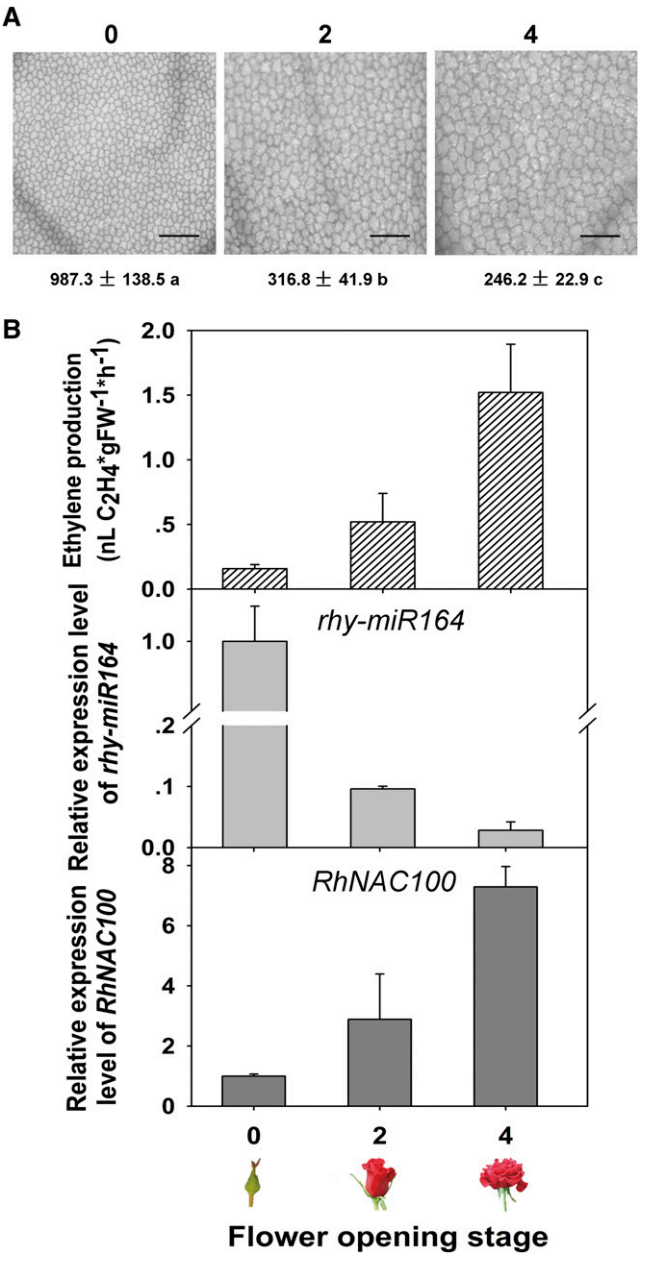

Figure 3. Changes in petal cell density, ethylene production, and expression of *rhy-miR164* and *RhNAC100* in rose petals during flower opening. A, Petal cell density of AbsE. Each data point represents the mean ± SD ($n = 30$). Different letters indicate significant differences ($P < 0.05$) calculated using one-way ANOVA followed by Tukey's honestly significant difference test. 0, Unopened buds; 2, completely opened buds; 4, opened flowers. Bar = 200 μm. The cells were counted in visual fields of 1,024 × 1,024 μm. B, Ethylene production (top) and expression profiles of *rhy-miR164* (middle) and *RhNAC100* (bottom) in rose petals during natural flower opening. The qRT-PCR was performed using at least three biological replicates. The internal controls used were 5S rRNA and *RhACT5* for *rhy-miR164* and *RhNAC100*, respectively. [See online article for color version of this figure.]

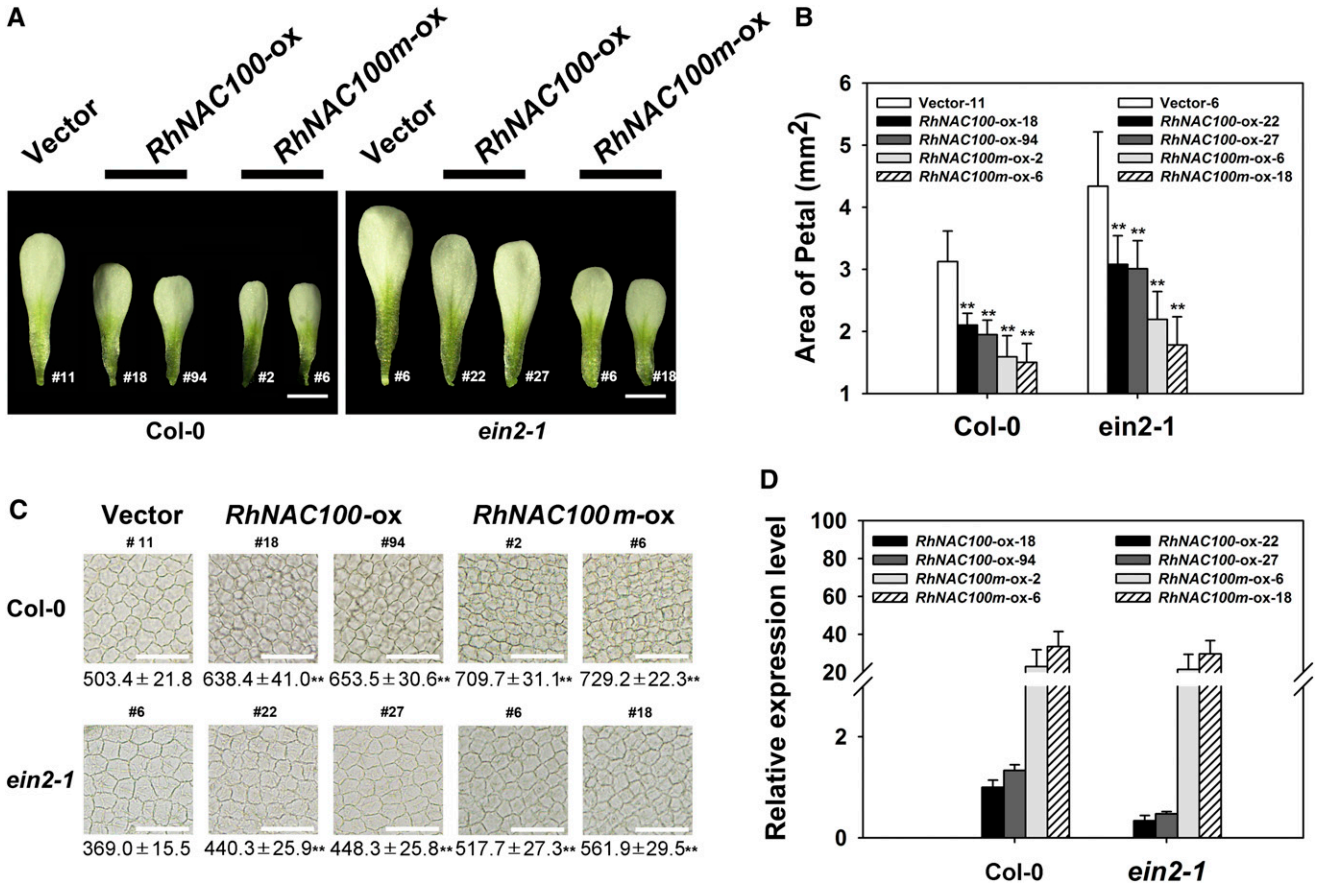

Figure 4. Petal phenotype of transgenic Arabidopsis overexpressing *RhNAC100* and *RhNAC100m*. A, Petal phenotype of *RhNAC100*-ox and *RhNAC100m*-ox with a Col-0 (left) and *ein2-1* (right) background. Bar = 200 μm. B, Statistical analysis of petal size of transgenic plants. The bars indicate the SD ($n > 15$ for each line). **Student's *t* test, $P < 0.01$. C, Cell density in petals from transgenic Arabidopsis plants. Petals of stage-14 flowers were fixed using formaldehyde-acetic acid and cleared by ethanol. The distal portion of the petal epidermis was used to analyze the cell number because this portion contains cells that are diploid and uniform in size (Mizukami and Fischer, 2000). The images of abaxial epidermal cells were taken by using a Nikon IX-71. Cell numbers were counted per visual field using ImageJ software. At least 15 flowers were used for each line. Bar = 50 μm. **Student's *t* test, $P < 0.01$. D, Expression of *RhNAC100/RhNAC100m* in transgenic plants. The qRT-PCR was performed using at least three biological replicates. *ACTIN2* was used as the internal control. Bars indicate the SD.

RhNAC100. Therefore, we analyzed the expression level of transgene *RhNAC100/RhNAC100m* to confirm whether it is related to the phenotype. *RhNAC100* and *RhNAC100m* were detected by qRT-PCR using the same primers that were designed across the *miR164*-binding site.

qRT-PCR demonstrated that, compared with *RhNAC100*/Col (#18) plants, expression of the *RhNAC100* transgene was 33.8% to 47.2% in *RhNAC100/ein2*, while expression of the *RhNAC100m* was 23.0- to 33.5-fold and 21.5- to 29.7-fold in *RhNAC100m*/Col and *RhNAC100m/ein2* plants, respectively (Fig. 4D). Interestingly, although the expression level of *RhNAC100* was much lower in the *RhNAC100/ein2* lines than in *RhNAC100*/Col, expression level of *RhNAC100m* was similar between the *RhNAC100m/ein2* and *RhNAC100m*/Col lines, which is consistent with the results presented in Figure 2C. These results indicated that expression level of the *RhNAC100* transgene is inversely correlated with petal size but positively correlated with abaxial epidermal cell density in transgenic Arabidopsis. The overexpression of *RhNAC100* was also observed, and *RhNAC100m* significantly decreased the length of hypocotyls and roots, as well as leaf size in transgenic plants ($P < 0.05$, Tukey's test), particularly in *RhNAC100m*-ox lines (Supplemental Fig. S5). Surprisingly, overaccumulation of *RhNAC100* transcripts repressed the elongation of hypocotyls in transgenic plants with Col-0 and ethylene-insensitive *ein2* backgrounds. These results further indicate that *RhNAC100* may function as a TF downstream of the ethylene signal.

The role of *RhNAC100* was also investigated in rose petal expansion using a virus-induced gene silencing (VIGS) approach (Ma et al., 2008; Spitzer-Rimon

et al., 2010; Jia et al., 2011). The *RhNAC100*-specific 3′-untranslated region was chosen to construct a TRV (Tobacco Rattle Virus)-*RhNAC100* vector to specifically silence *RhNAC100* in rose petals (Fig. 5A). Compared with TRV petals (14.83 ± 1.46 cm^2), *RhNAC100*-silencing significantly increased petal size (by approximately 19.3%) to 17.68 ± 1.58 cm^2 ($P < 0.05$; Fig. 5B). To determine whether the close homologs of *RhNAC100* were also silenced, we developed gene-specific primers to test the transcript abundance of homologous *NAC* genes in *RhNAC100*-silenced and TRV-infected petals, including RU20317, RU01707, RU04695, RU026684, and RU26219, which are close homologs of *RhNAC100* (Supplemental Fig. S6A). No reductions in transcript abundance were detected (Supplemental Fig. S6B). Therefore, although the possibility cannot be completely excluded that some closely related homologs were down-regulated, these data verify a high degree of target specificity in our VIGS experiments.

In our previous research, we observed that ethylene inhibits cell expansion in the petal AbsE, particularly in the upper petal regions (Ma et al., 2008). Therefore, it was examined whether *RhNAC100* influences cell expansion in the upper petal region. Silencing of *RhNAC100* resulted in a significantly decreased number of AbsE cells per microscope visual field, from 181.9 ± 11.8 in TRV petals to 138.9 ± 10.8 in *RhNAC100*-silenced petals ($P < 0.05$, Tukey's test), which is a decrease of approximately 23.6% (Figs. 5, C and D). These results suggest that *RhNAC100* plays an important role in ethylene-regulated inhibition of petal cell expansion.

RhNAC100 Regulates a Subset of Genes Involved in Cell Expansion

To investigate how *RhNAC100* regulates cell expansion in transgenic Arabidopsis, the potential downstream target genes of *RhNAC100* were explored by microarray analysis using the ATH1 Genome Array. Overaccumulation of *RhNAC100* transcripts in transgenic Arabidopsis plants (*RhNAC100m*-ox/Col) resulted in significant changes in the expression of 549 genes (164 up-regulated and 385 down-regulated), including genes related to cell wall catabolism/organization, water and solute transportation, and cytoskeleton remodeling (Supplemental Table S5). We chose 29 cell expansion-related rose genes based on their homology with the changed Arabidopsis genes in the *RhNAC100m*-ox plant and quantified their expression in *RhNAC100*-silenced petals. The expression levels of 22 out of the 29 genes tested were altered following *RhNAC100* silencing, and 19 out of those 22 exhibited an inverse expression patterns compared with their homologs in the *RhNAC100m*-ox/Col Arabidopsis plants (Table I). In addition, the expression of these 29 genes were tested in the petals during flower opening. The result showed that most exhibited a substantial change in expression upon flower opening

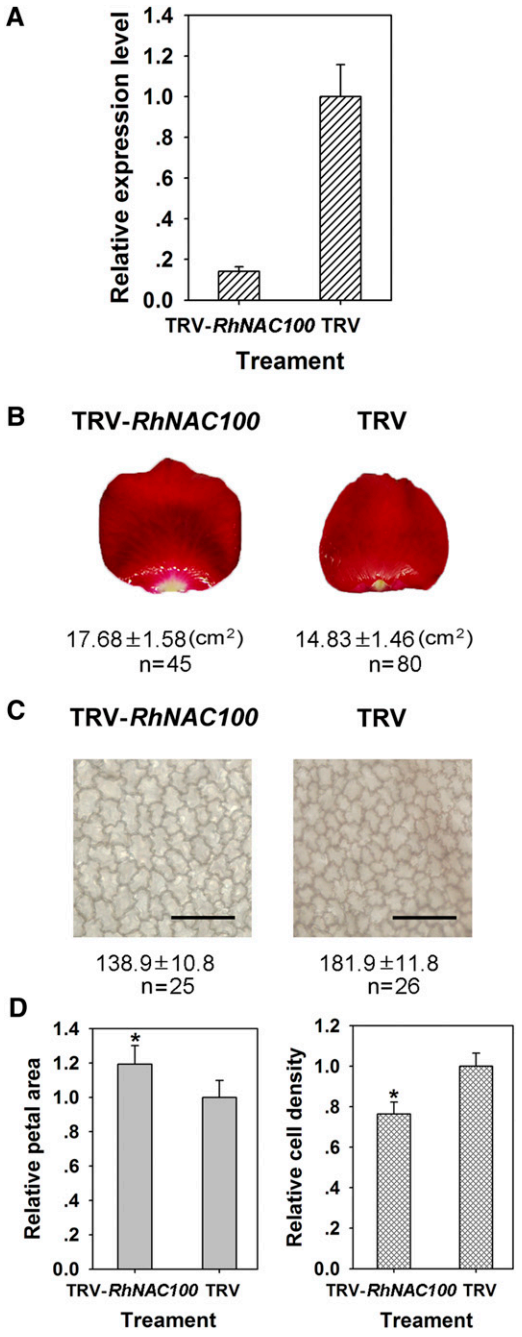

Figure 5. Silencing of *RhNAC100* in rose petals by VIGS. A, The qRT-PCR analysis of *RhNAC100* in *RhNAC100*-silenced petals. *RhACT5* was used as the internal control. TRV, Empty vector; TRV- *RhNAC100*, TRV containing a fragment of *RhNAC100*; control, petals without infiltration. B, Size of *RhNAC100*-silenced petals. These photographs were taken 8 d after infiltration. Each data point indicates the mean ± SD. Six independent experiments were performed; at least 80 petals were used for each treatment per experiment. C, Cell density of AbsE of *RhNAC100*-silenced petals. Bar = 200 μm. Each data point represents the mean ± SD. Different letters indicate significant differences ($P < 0.05$) calculated using one-way ANOVA followed by Tukey's honestly significant difference test. The cells were counted using visual fields of 1,024 × 1,024 μm. D, The relative petal area and cell density. The petal area and cell density of TRV petals was set to 1.

Table I. *qRT-PCR analysis of 29 putative downstream genes of RhNAC100 in RhNAC100-silenced rose petals comparing with TRV (petals infiltrated by empty vector)*

Gene Family	ID	Expression Changed Fold	SD
NAC domain TF	*RhNAC100*	0.08	0.003
Cellulose synthase-like protein	*RU04718*	8.01	0.760
	RU23321	3.32	0.722
	RU01568	2.41	0.047
	RU05842	1.17	0.039
Cellulase	*RU22926*	4.51	0.480
	RU04698	0.92	0.106
β-1,3-glucanase-like protein	*RU05209*	0.12	0.033
Endoxyloglucan transferase	*RU00964*	8.04	0.427
	RU04847	7.62	0.290
	RU06454	14.64	2.053
Expansin	*RU05224*	2.38	0.155
Extensin	*RU02382*	9.75	0.221
Pectinesterase	*RU03736*	3.44	0.032
Xyloglucan endotransglycosylase-related protein	*RU00040*	6.20	0.625
	RU10722	1.81	0.029
	RU19414	9.90	3.620
	RU20002	11.66	2.738
Aquaporin	*RhPIP1;1*	7.05	0.047
	RhPIP2;1	9.46	0.172
	RU34590	0.99	0.083
Sugar transporter	*RU04906*	0.65	0.044
	RU08526	0.11	0.032
	RU04803	1.51	0.452
Putative microtubule protein	*RU20999*	4.15	0.388
Actin depolymerizing-factor-like protein	*RU03106*	0.57	0.160
	RU06169	1.41	0.205
Formin	*RU04247*	0.11	0.018
Kinesin	*RU05467*	6.66	0.773
Profilin	*RU22810*	1.15	0.195

(Supplemental Table S6). However, whether these genes are involved in petal development needs to be further tested.

Of the cell wall-related genes, the genes encoding cellulose synthases were focused on because our pathway analysis showed that the cellulose synthetic pathway, which is primarily governed by cellulose synthases, changed significantly following ethylene treatment of rose petals (adjusted *P* value, 0.00277; Supplemental Table S7). In this pathway, one of the cellulose synthase genes (*RU04718*) was strongly repressed following ethylene treatment (Supplemental Table S8), whereas the levels of *RU04718* transcript increased substantially in *RhNAC100*-silenced rose petals (Table I). The open reading frame of RU04718 is 3,285 bp in length and encodes a putative cellulose synthase of 1,094 amino acids. This gene was designated *RhCesA2* because its closest homolog is *CESA2* in Arabidopsis and has been deposited in GenBank with the accession number JQ001775. Phylogenetic analysis showed that *RhCesA2* is closely related to the CESA2/CESA5/CESA6/CESA9 subclade of 10 CESA proteins from Arabidopsis (Supplemental Fig. S7A), and the expression of *RhCesA2* was repressed by ethylene treatment of rose petals (Supplemental Fig. S7B). To test whether *RhCesA2* is a direct downstream target gene of RhNAC100, we isolated the promoter of *RhCesA2* and performed an electrophoretic mobility shift assay (EMSA). A previous report showed that NAC protein is capable of binding the core sequence CGT[G/A] or its reverse complementary sequence [C/T]ACG (Tran et al., 2004; Olsen et al., 2005; Balazadeh et al., 2010; Hao et al., 2011). Biotin-labeled DNA probes were designed based on the region –354 to –324 bp upstream of *RhCesA2*, which contains the core sequence CGTG. Because the N-terminal domains of NAC proteins possess DNA-binding activity, a GST (Glutathione *S*-transferase)-RhNAC100-N recombinant protein was generated containing the N terminus of RhNAC100 (1–171 amino acids) fused to a GST tag. As shown in Figure 6, two bands were detected using this assay, which may correspond to the RhNAC100 homodimer-DNA complex (top band) and the RhNAC100 monomer-DNA complex (bottom band) that is frequently associated with NAC proteins when they bind the promoter of a target gene (Yamaguchi et al., 2011). Shifted bands were detected when the GST-RhNAC100-N recombinant protein was combined with biotin-labeled DNA probes, whereas no shifted bands were detected when a GST control protein was combined with a biotin-labeled DNA probe. The protein/DNA-binding bands showed a decreasing

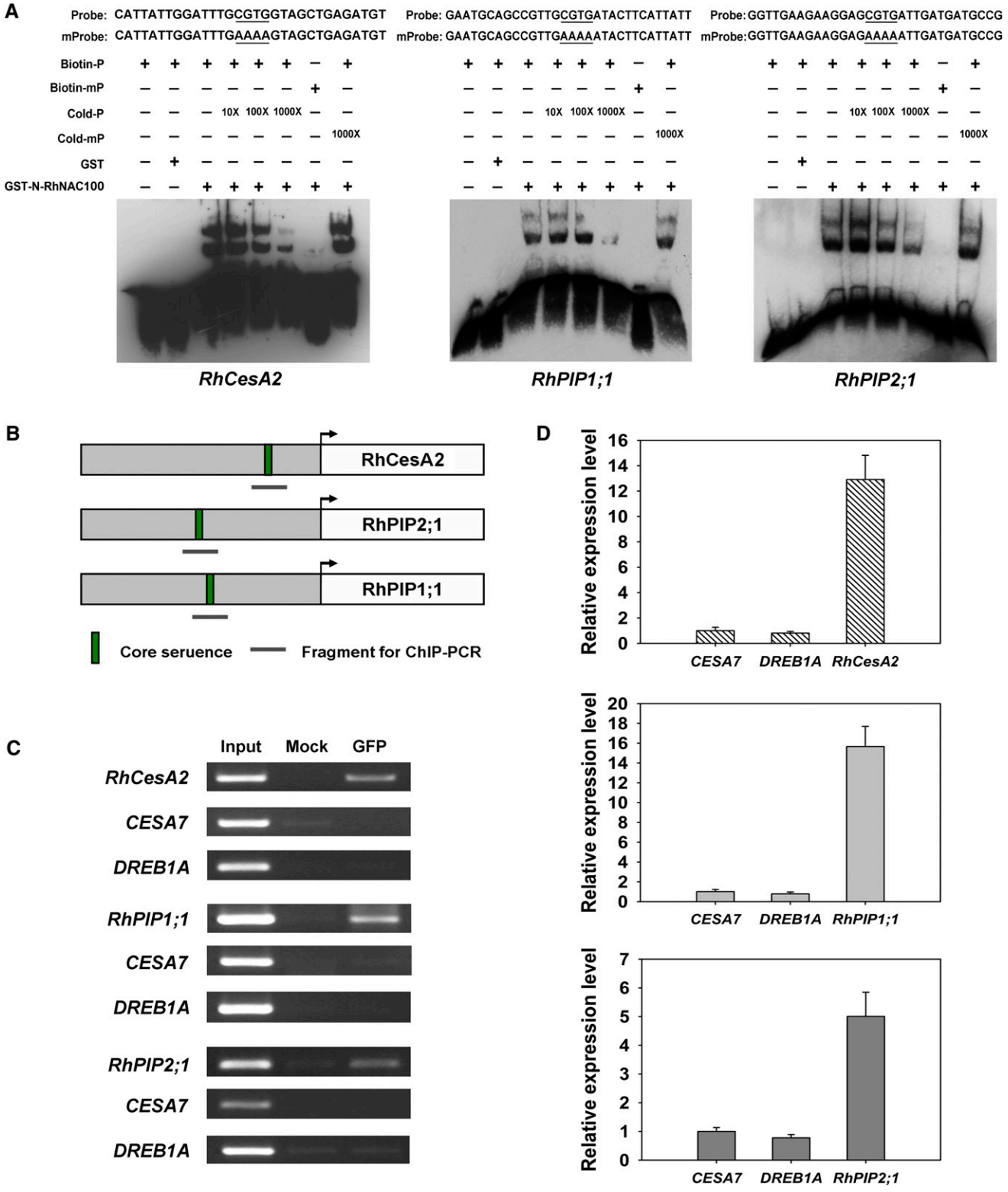

Figure 6. Binding test of RhNAC100 to promoters of its downstream targets in vitro (A) and in vivo (B–D). A, Gel-shift analysis of RhNAC100 N terminus binding to *RhCesA2*, *RhPIP1;1*, and *RhPIP2;1* promoters. Purified protein (1 μg) was incubated with 25 picomoles biotin-labeled probes or mutant probes (mP). For the competition test, nonlabeled probes at varying concentrations (from 10- to 1,000-fold excess) or labeled mutant probes (1,000-fold) were added to the above experiment. B, Schematics of the promoter sequences of *RhCesA2*, *RhPIP1;1*, and *RhPIP2;1*. The core sites and regions used for the ChIP assays are

signal as the concentration of cold competitor DNA probes increased. However, the GST-RhNAC100-N protein did not bind to the biotin-labeled and mutated DNA probe, and a 1,000-fold excess of unlabeled and mutated probes was incapable of weakening the binding of the GST-RhNAC100-N protein to the labeled probes (Fig. 6A). These results indicate that RhNAC100 binds to the promoter of *RhCesA2*. In addition, the core sequence CGT[G/A] was noted in the promoter of two aquaporin genes, those of *RhPIP1;1* (CGTG) and *RhPIP2;1* (CGTG; ACE60220). RhNAC100 is capable of binding to the promoters of *RhPIP1;1* and *RhPIP2;1* (Fig. 6A). To confirm the binding of RhNAC100 to promoters of downstream genes in vivo, a chromatin immunoprecipitation (ChIP) assay was performed using mesophyll protoplasts of transgenic Arabidopsis plants expressing Pro*RhCesA2*:*GUS*, Pro*RhPIP1;1*:*GUS*, or Pro*RhPIP2;1*:*GUS*. The protoplasts were transfected with *35S*:*RhNAC100-GFP*. RhNAC100 binding fragments were enriched following immunoprecipitation with an anti-GFP antibody. Promoter fragments containing the core sequence of all three downstream genes, *RhCesA2*, *RhPIP1;1*, and *RhPIP2;1*, were enriched (Fig. 6, B–D), indicating that RhNAC100 can bind to the promoters of *RhCesA2*, *RhPIP1;1*, and *RhPIP2;1* in vivo.

The silencing of *RhPIP1;1* (Chen et al., 2013) or *RhPIP2;1* (Ma et al., 2008) substantially inhibited abaxial epidermal cell expansion in rose petals. To investigate whether *RhCesA2* is also involved in rose petal expansion, *RhCesA2* was silenced in rose petals using a 377-bp *RhCesA2*-specific fragment using the VIGS approach. Silencing of *RhCesA2* decreased the petal area by 13.6% and increased the AbsE cell density by 16.2% in the upper petal region compared with the TRV control (Supplemental Fig. S7, C–F; $P < 0.05$, Tukey's test).

DISCUSSION

Floral Transcriptome and Ethylene-responsive Profiles in Rose Petals

Despite the economic and cultural importance of rose, genomic resources for this crop species are relatively limited. During the past decade, genomics approaches have been applied in rose, and several EST libraries from rose petals were reported (Channeliére et al., 2002; Guterman et al., 2002; Bendahmane et al., 2013). In 2008, approximately 10,000 ESTs were deposited in public databases, including GenBank and Genome Database for the Rosaceae (http://www.rosaceae.org/). Based on these data, expression profiles of 4,765 transcripts were detected in rose from floral transition to flower senescence using a newly developed Affymetrix microarray (Dubois et al., 2011). Moreover, application of next-generation sequencing technologies greatly promoted the study on rose genomics. A rose transcriptome database was reported recently, which contained more than 30,000 transcripts from three modern rose cultivars and *Rosa rugosa* (Kim et al., 2012). Lately, a transcriptome data set containing 80,714 transcript clusters was generated by using the RNA from various tissues of *Rosa chinensis* 'Old Blush' and in response to biotic and abiotic stresses (Dubois et al., 2012).

In this work, using 454 technology, approximately 300,000 high-quality rose transcript sequences were generated, which were further assembled into 60,944 unique transcripts, providing a valuable resource for rose functional genomic studies.

In Arabidopsis, the expression of approximately 4% of genes are significantly affected by ethylene, including genes involved in plant defense, ethylene biosynthesis and signaling, and cell wall biosynthesis and degradation (De Paepe et al., 2004). In tomato pericarp, *Never ripe*, an ethylene insensitive mutation, leads to significant changes in expression patterns of 607 genes, including those involved in protein synthesis and primary metabolic processes (Alba et al., 2005). Here, in rose petals, we obtained 2,189 ethylene-responsive transcripts. Annotation of these transcripts indicated that cell expansion-related processes, such as cell wall synthesis, cell turgidity, and cytoskeleton remodeling, were significantly affected by ethylene treatment.

Multiple hormones largely contribute to similar biological processes (Jaillais and Chory, 2010). Here, we demonstrated that ethylene influences the expression of several TFs and regulator genes that are involved in the signaling of auxin (e.g. ARF and AUX/IAA), gibberellin (e.g. DELLA), and brassinosteroid (e.g. BEE). Recently, a report showed that ARF8 interacted with BIGPETALp, a bHLH TF, to regulate both cell proliferation and expansion, ultimately affecting petal size in Arabidopsis (Varaud et al., 2011). In addition, microarray analysis showed that expression of two AUX/IAA genes, one ARF gene, and one Brassinosteroid-regulated protein (Brassinosteroid Upregulated Protein1) gene were significantly altered during flower opening of *Rosa* spp. (Dubois et al., 2011). The integration of these hormonal signals into a model of petal growth requires further investigation.

Figure 6. (*Continued.*)
indicated. C, ChIP assay of *RhCesA2*, *RhPIP1;1*, and *RhPIP2;1* promoters. *ProRhCesA2*:*GUS*, *ProRhPIP1;1*:*GUS*, and *ProRhPIP2;1*:*GUS* transgenic plants grown on soil for 3 weeks were used to extract leaf mesophyll protoplasts. *35S*:*RhNAC100-GFP* plasmid was transfected into the protoplast of each line. Three independent experiments were performed with each showing similar results. *CESA7* and *Dehydration Responsive Element Binding Factor1A* (*DREB1A*) were included in this experiment as controls. D, qRT-PCR of the ChIP assay described in C. For ChIP assays (bottom), three replicates were averaged for each individual assay. Bars indicate the SD. [See online article for color version of this figure.]

The *miR164/RhNAC100* Module Is Involved in Ethylene-Regulated Cell Expansion

In rose flowers, ethylene can reduce the petal size, which is associated with increased AbsE density (Ma et al., 2008). Here, an ethylene-inducible NAC TF gene, *RhNAC100*, was identified in rose petals. Silencing of *RhNAC100* in rose significantly increased the petal size and decreased the AbsE cell density, indicating that RhNAC100 plays an important role in mediating the ethylene signal to modulate cell expansion. However, our results also indicated that RhNAC100 might be involved in cell proliferation too, because the petal size change (approximately 50%) in *RhNAC100m*-ox/Col transgenic plant is larger than the change in density of abaxial epidermal cells (approximately 40% increase). Conversely, qRT-PCR showed that the level of *RhNAC100* transcript is low during the early stages of petal opening (stages 0 and 2), when growth is mainly driven by cell division (Yamada et al., 2009). Therefore, despite that *RhNAC100* might be able to affect cell proliferation, it could not substantially affect the cell proliferation in natural developmental progress in rose petals.

Meanwhile, the possibility cannot be ruled out that other factors may act synergistically with RhNAC100 to regulate cell expansion. Given that at least 105 TFs are responsive to ethylene in rose petals, it is likely that other TFs may also be involved in ethylene-regulated cell expansion.

In Arabidopsis, a subset of NAC TFs is targeted by the well-conserved *miR164* family (Jones-Rhoades and Bartel, 2004; Sieber et al., 2007). Although the *miR164*-targeted site and the mechanism of *miR164*-mediated cleavage are conserved, *miR164* can participate in various development processes by targeting different *NAC* genes. In Arabidopsis roots, the *miR164/NAC1* module is involved in lateral root initiation (Guo et al., 2005). The *miR164/CUC1/CUC2* module governs meristem initiation and organ separation and postembryonic boundary maintenance by primarily controlling the cell division process in shoots of Arabidopsis (Jones-Rhoades and Bartel, 2004; Laufs et al., 2004; Peaucelle et al., 2007; Raman et al., 2008). Overaccumulation of the *miR164*-resistant version of *CUC2* mRNA results in a longer period of cell proliferation (Peaucelle et al., 2007; Larue et al., 2009). Interestingly, the *miR164/CUC2* module is also considered to influence cell elongation in internodes during inflorescence development. *CUC2* can preserve cell proliferation but represses cell elongation during embryogenesis in Arabidopsis. *MiR164* is thought to cleave *CUC2* transcripts in internode cells to enable rapid growth of the internode at later stages of inflorescence development (Peaucelle et al., 2007). However, in rose petals, *miR164/RhNAC100* regulates cell expansion differently. In early period of flower opening (stages 0–2), levels of *miR164* are high, thereby preventing the accumulation of *RhNAC100* transcripts in petals and ensuring rapid cell expansion and petal growth. Later (stages 2–4), miR164 abundance decreases as ethylene production increases, resulting in an accumulation of RhNAC100, which restricts cell expansion and slows the rate of petal growth. These different modes of action indicate that temporal and/or spatial-specific expression patterns contribute to the diverse roles of *miR164* during multiple developmental events. The possibility cannot be also ruled out that *RhNAC100* may be regulated by multiple factors at both the transcriptional and posttranscriptional level. *RhNAC100* also influences the organ size of hypocotyls, roots, and leaves in transgenic Arabidopsis, but further investigation is necessary to clarify whether the miR164/RhNAC100 module is involved growth of other organs in rose.

Some miRNAs have been implicated in the regulatory network of several phytohormones, such as abscisic acid and GA (Rhoades et al., 2002; Achard et al., 2004; Jones-Rhoades and Bartel, 2004; Sunkar and Zhu, 2004; Khraiwesh et al., 2012). The *miR164/ORE1* (*ANAC092/AtNAC2*) miRNA regulates aging-induced cell death in leaves of Arabidopsis and can be influenced by mutating *EIN2* (Kim et al., 2009). In rose petals, ethylene greatly reduces the abundance of *miR164* while increasing the levels of *RhNAC100* (Fig. 2). It has been demonstrated that a loss-of-function mutation in *EIN2* leads to an increase in *miR164* abundance in Arabidopsis leaves (Kim et al., 2009). The *miR164*-directed cleavage of *RhNAC100* transcripts was substantially enhanced in transgenic Arabidopsis of an *ein2-1* background, whereas cleavage of the *miR164*-resistant version of *RhNAC100* was undetected in both Col-0 and *ein2-1* plants. All of these results indicate that ethylene may fine-tune the balance between *miR164* and *RhNAC100*.

Here, the abundance of *miR164* was increased by auxin and GA, and the expression of *RhNAC100* was suppressed by auxin and GA (Supplemental Fig. S3). Therefore, the balance between *miR164* and *RhNAC100* may be influenced by multiple hormones rather than solely by ethylene in rose petals. To date, auxin is known to regulate *miR164*, while it is unclear whether GA can regulate *miR164*. In Arabidopsis roots, auxin is capable of increasing the abundance of *miR164*, which targets *NAC1* and consequently inhibits lateral root initiation (Guo et al., 2005). In Arabidopsis leaves, a CINCINNATA-like TF, TEOSINTE BRANCHED1, CYCLOIDEA, and PCF3, directly activates the expression of *MIR164*, *ASYMMETRIC LEAVES1*, and auxin response repressor gene *IAA3/SHORT HYPOCOTYL2*, which cooperatively repress the accumulation of *CUC* gene transcripts (Koyama et al., 2007). However, there is no evidence to show how ethylene and auxin interact to regulate *miR164*. Interestingly, ethylene is known to work with auxin synergistically during plant development, although ethylene typically acts as an antagonist to auxin (Pierik et al., 2006). Ethylene stimulates auxin biosynthesis and basipetal auxin transport to zones of elongation (Růzicka et al., 2007), and the effects of ethylene on the inhibition of

cell elongation in elongation zones are enhanced when auxin is present (Swarup et al., 2007). By contrast, the functions of auxin or ethylene on root inhibition are partially overlapped. In particular, some ethylene-mediated inhibition of root growth is auxin independent (Stepanova et al., 2007; Swarup et al., 2007). Meanwhile, ethylene is capable of modulating the bioactive level of GA and the protein stability of DELLA proteins, including GIBBERELLIC-ACID INSENSITIVE and REPRESSOR OF GA1-3 in Arabidopsis (Achard et al., 2003; Achard et al., 2007; Vandenbussche et al., 2007; Weiss and Ori, 2007). Here, *miR164* abundance was increased by GA, whereas the expression of *RhNAC100* was reduced in rose petals. It remains unclear whether the effects on the *miR164/RhNAC100* module by GA are ethylene dependent. Notably, cross regulation by ethylene, auxin, and GA is highly tissue specific (Yoo et al., 2009; Muday et al., 2012). For example, ethylene and GA have antagonistic roles in the floral meristem to modulate floral transition (Achard et al., 2007), whereas ethylene-induced formation of the apical hook requires GA and auxin in etiolated seedlings (Vriezen et al., 2004; Stepanova et al., 2008). Therefore, the type of cross regulation by ethylene, auxin, and GA that occurs in rose petals and whether *miR164* functions as a mediator to integrate these hormone signals require further study.

RhNAC100 Regulates the Expression of Cell Expansion-Related Genes

Cell expansion is a comprehensive biological process requiring a highly efficient coordination of cell wall growth, turgor modulation, and cytoskeleton remodeling. Here, we found that the expression level of 22 functional genes that may participate in the cell expansion was affected by *RhNAC100* in rose petal. Three of these genes, two aquaporin (*RhPIP1;1* and *RhPIP2;1*) genes and one cellulose synthase gene (*RhCesA2*), were identified as the possible direct downstream genes of RhNAC100 both in vitro and in vivo.

During the cell expansion process, enlargement in cell volume is driven by cellular water uptake, which results from turgor relaxation accompanied by a loosening of the cell wall. Aquaporin serves as the primary channel enabling water uptake across biological membranes. Previously, we observed that two plasma aquaporins, *RhPIP2;1* and *RhPIP1;1*, are involved in cell expansion (Ma et al., 2008; Chen et al., 2013). Our current results imply that RhNAC100 is likely to be involved in turgor modulation.

However, the role of *RhNAC100* in cell wall loosening and synthesis is unclear. Previously, several NAC genes from the *VND/NST/SND1* subfamily were reported to regulate cellulose synthases involved in the cellulose synthesis of the secondary cell wall (Mitsuda et al., 2005; Zhong et al., 2006, 2010; Ko et al., 2007). A recent report showed that cell wall-related genes were highly enriched and up-regulated in the *atnac2/anac092/ore1* mutant, indicating that *ANAC092/AtNAC2/ORE1* plays a role in the modification of the cell wall (Balazadeh et al., 2010). In addition, based on the current model, different CESA proteins form a rosette complex to facilitate the synthesis of cellulose, and the cellulose in the primary and secondary cell walls is synthesized by different sets of cellulose synthases. Deposits of cellulose in the secondary cell wall but not in the primary cell wall typically arise when the cell stops expanding and results in a restriction of cell growth. In *Arabidopsis*, *CESA2*, *CESA5*, *CESA6*, and *CESA9* contribute to cellulose synthesis for the primary cell wall, whereas *CESA4*, *CESA7*, and *CESA8* contribute to cellulose synthesis for the secondary cell wall (Taylor, 2008).

Here, RhNAC100 was able to bind to the promoter of *RhCesA2* and probably suppressed the expression of *RhCesA2*, a homolog of Arabidopsis *CESA2*. The *cesa2* mutant exhibits stunted growth of hypocotyls due to reduced cell expansion caused by a defect in cellulose synthesis (Chu et al., 2007).

Notably, our current data are insufficient to provide a complete view of the role of RhNAC100 during cell expansion. The 29 genes that were tested in this study represent only a small fraction of the total possible number of genes involved because many other genes could be involved in cell expansion. For instance, we noted that the expression of four xyloglucan endotransglucosylase/hydrolase (XTH) genes decreased in *RhNAC100*-silenced petals, whereas they showed different patterns and levels of expression during the flower opening (Table I). XTH is a large gene family and is thought to be involved in varying, and in some cases opposing, functions, such as wall loosening, wall strengthening, the integration of new xyloglucans into the wall, and the hydrolysis of xyloglucans (Cosgrove, 2005). Thus, it will be necessary to confirm the actual XTH genes are downstream to RhNAC100 and to clarify their actual function in petal cell expansion. In addition, it would be interesting to investigate whether other cell wall growth-related proteins, such as expansin, pectin methylesterase, and endo-(1,4)-β-D-glucanase, are also involved in ethylene-regulated cell expansion. When rose genome becomes available, a chromatin-immunoprecipitation followed by massively parallel sequencing assay will assist in establishing the *RhNAC100*-dependent regulatory network involved in cell expansion.

*miR164/NAC*s Might Be Conserved Module for Petal Development

Petal development is an important process for life cycle in most higher plants. In present work, an NAC TF gene, *RhNAC100*, was found to be able to regulate petal expansion in rose. In addition, overexpression of *RhNAC100* also influenced petal size in transgenic Arabidopsis in a *miR164*-dependent manner. In

Arabidopsis, although the exact function of *ANAC100* (AT5G61430), the closet homolog of *RhNAC100*, is still unknown, two homologs, *CUC1* and *CUC2*, were found to be involved in petal initiation and petal number decision (Aida and Tasaka, 2006). Similarly, mutation of *miR164* also resulted in abnormal petal number and phenotype (Mallory et al., 2004; Baker et al., 2005; Sieber et al., 2007). Considering that *miR164* is highly conserved in plants, the *miR164/NAC* module might play a conserved role in petal development in plants, although different NAC members probably function in different petal development phases, such as petal initiation, petal expansion, etc.

In conclusion, we created a rose floral transcriptome and exploited it to identify the potential key regulators for ethylene-influenced cell expansion. We identified an NAC domain TF, *RhNAC100*, whose expression is highly inducible by ethylene. *RhNAC100* is a negative regulator for petal cell expansion in rose and is able to influence petal growth when overexpressed in Arabidopsis. Detailed genetic and biochemical analysis revealed that *RhNAC100* was a target of *miR164* and that ethylene elevated the accumulation of *RhNAC100* transcript by blocking *miR164*-guided cleavage of *RhNAC100*. *RhNAC100* regulated genes related to cell expansion, such as cellulose synthase and water transporter (aquaporin). We provide evidence for a TF/miRNA-based genetic pathway in the control of cell expansion by ethylene.

MATERIALS AND METHODS

Plant Materials

Flowers were harvested from rose (*Rosa hybrida*) 'Samantha' at stage 2 of floral opening (Ma et al., 2005). The flowers were immediately placed in tap water after harvesting and transported to the laboratory within 1 h. After cutting to 25-cm lengths under water, the flowers were placed in deionized water. The flowers were treated with 10 μL L^{-1} ethylene and 2 μL L^{-1} 1-MCP in a sealed airtight chamber, and flowers exposed to air were used as a control. Treatments were conducted at 23°C to 25°C, and 1 mol L^{-1} NaOH was included in the chamber to prevent the accumulation of CO_2 (Ma et al., 2006). Treatment time points were 0, 0.5, 1, 2, 6, 12, 18, 24, and 48 h for the 454 transcriptome sequencing and 0, 1, 6, 12, 18, and 24 h for microarray analysis.

Arabidopsis (*Arabidopsis thaliana*) seeds were surface sterilized, plated on Murashige and Skoog medium, and imbibed in the dark at 4°C for 2 d. The plates were transferred to a growth room maintained at 21°C to 22°C at 60% relative humidity under a 16-h-light/8-h-dark photoperiod. After 7 d, seedlings were transplanted in pots containing a 1:1 mixture of vermiculite and peat moss and grown under the same conditions. For ethylene treatment, 2-week-old Arabidopsis seedlings were exposed to 10 μL L^{-1} ethylene for 24 h in an airtight chamber. For naphthaleneacetic acid (NAA), GA, and brassinosteroid treatments, roses at stage 2 were treated with 20 μM NAA, 25 μM, or 10 μM brassinosteroid for 24 h at 23°C to 25°C. Mock samples were treated with dimethyl sulfoxide without any phytohormones.

Microarray Construction, Hybridization, and Data Analyses

The unisequences were selected for designing the microarray primarily based on their annotations, digital expression patterns, and abundance obtained from the corresponding EST counts.

First, the unisequences were screened by digital expression patterns and corresponding EST counting. Digitally differential expression was computed by comparison of reads from ethylene-treated rose flowers and untreated controls using IDEG6 software (Romualdi et al., 2003). The results were tested using a Fisher exact test with Bonferroni correction, and 5,652 unisequences were selected. Second, all unisequences that were annotated as regulatory factors, such as TF, TR, kinase, and phosphatase, were selected, regardless of their digital expression patterns and corresponding EST counting, and 10,922 unisequences were selected. Based on the total number of selected unisequences (16,574), we chose the Agilent 8X15 K microarray format. All 16,574 unisequences were sent to Agilent to design probes using eArray (https://earray.chem.agilent.com/earray/). Probe designs failed for a total of 1,577 unisequences due to their short length and low sequence specificity, leaving a total of 14,997 unisequences in the final probe set.

Cy3-labeled cDNA samples were denatured independently and used for the microarray assay. All hybridizations used three biological replicates with only one exception; the hybridization of the 12-h ethylene-treated sample was conducted for only two biological replicates. Fluorescence intensities on the scanned images were quantified. The resulting values were corrected for background nonspecific hybridization and normalized using the quantile normalization method (Bolstad et al., 2003). Differentially expressed genes between ethylene-treated and control flower petals at each time point were identified using the moderated *t* statistics in the LIMMA package (Bolstad et al., 2003). Raw *P* values were adjusted for multiple testing using the FDR (Benjamini and Hochberg, 1995). Genes with FDR of less than 0.05 and fold changes in expression of at least 2 were considered differentially expressed genes. Differentially expressed genes were clustered using Cluster 3.0 (de Hoon et al., 2004) using the average linkage method and, the Pearson correlation was used as the distance metric. The clustered gene expression profiles were visualized using Treeview (Eisen et al., 1998). GO, biochemical pathway, and differential expression data sets were imported into the Plant MetGenMAP system (Joung et al., 2009) to identify significantly changed pathways (adjusted *P* value < 0.05). The entire microarray data set has been deposited into the rose transcriptome database (http://bioinfo.bti.cornell.edu/rose).

For possible downstream gene screening of *RhNAC100*, total RNA from Arabidopsis wild-type Col-0 and transgenic plants overexpressing *RhNAC100*/*RhNAC100m* was extracted and labeled, and hybridization was performed using the Affymetrix ATH1 Genome Array.

Sequence Analysis

Alignment of the amino acid sequence and phylogenetic analysis was performed using ClustalW and MEGA 4.0, respectively. The phylogenetic trees were computed using the neighbor-joining algorithm with 10,000 bootstrap replicates.

qRT-PCR

For qRT-PCR, 1 μg of DNase-treated RNA was used to synthesize cDNA according to the manufacturer's instruction for the reverse transcription system (Promega) using a 25-μL reaction volume. Two microliters of cDNA was used as the template in a 20-μL PCR reaction, and the Bio-Rad CFX96 real-time PCR detection system was used in standard mode with the Bio-Rad iQ SYBR-Green Supermix. Each reaction was performed in triplicate, and products were verified by melting curve analysis. The abundance of mRNA and miRNA was analyzed using the relative standard curve method normalized to *R. hybrida actin5* and *5S ribosomal RNA*, respectively. All reactions were performed with at least three biological replicates.

VIGS in Rose Petals

RhNAC100 silencing was performed as previously described (Ma et al., 2008). A 320-bp fragment at the 3′ end of *RhNAC100* was used to generate the pTRV2- *RhNAC100* construct. pTRV2-*RhNAC100*, pTRV1, and pTRV2 vectors were transformed into *Agrobacterium tumefaciens* GV3101. *A. tumefaciens* was grown in Luria-Bertani broth containing 50 μg mL^{-1} kanamycin and 50 μg mL^{-1} gentamycin sulfate at 28°C with shaking at 200 rpm overnight. These cultures were diluted 1:50 (v/v) in fresh Luria-Bertani broth containing 10 mM MES, 20 mM acetosyringone, 50 μg mL^{-1} kanamycin, and 50 μg mL^{-1} gentamycin sulfate and grown overnight as described above. *A. tumefaciens* cells were harvested by centrifugation at 4,000 rpm for 10 min and were suspended in infiltration buffer (10 mM $MgCl_2$, 150 mM acetosyringone, and 10 mM MES, pH 5.6) to a final optical density at 600 nm of approximately 1.5. A mixture of *A. tumefaciens*

cultures containing pTRV1 and pTRV2-*RhNAC100* at a ratio of 1:1 (v/v) and a mixture containing pTRV1 and pTRV2 at a 1:1 ratio (the negative control) were stored at room temperature for 4 h in the dark prior to vacuum infiltration. For vacuum infiltration, three to six pieces of petals were picked from the second and third whorl of each stage 1.5 flower, and they were randomly assigned to different treatments. For each treatment, at least 80 petals with six replicates were used. The petals were immersed in the bacterial suspension solution and infiltrated at a vacuum of 0.7 atm. After releasing the vacuum, the petals were washed with deionized water, maintained vertically in deionized water for 3 d at 8°C, and then transferred to 23°C for 5 d. Photos of the petals were taken daily, and petals were picked for RNA isolation on the eighth day after infiltration. Petal size was measured from the photos using ImageJ software. Statistical testing was performed using SPSS software.

Microscopic Examination and Cell Counting

For rose, AbsE cell photography and cell counting were performed as described previously (Ma et al., 2008). Briefly, discs of 3-mm diameter petal at 25% of the petal length from the petal top were taken. The discs were fixed in formaldehyde-acetic acid (3.7% [v/v] formaldehyde, 5% [v/v] glacial acetic acid, and 50% [v/v] ethanol) and cleaned using ethanol. AbsE cells from the discs were photographed using a Nikon IX-71 camera. For Arabidopsis, petals of stage-14 flowers were fixed using formaldehyde-acetic acid and cleared by ethanol. The distal portion of the petal epidermis was used to analyze the cell number because this portion contains cells that are diploid and uniform in size (Mizukami and Fischer, 2000). The images of abaxial epidermal cells were taken by using a Nikon IX-71 camera. Cell numbers were counted per visual field using ImageJ software.

Northern Hybridization

Northern blotting was performed as described previously (Ma et al., 2006). A gene-specific probe was generated using a PCR DIG Probe Synthesis Kit (Roche). Hybridization was performed overnight at 43°C. The chemiluminescent reaction was performed using CDP-Star according to the manufacturer's protocol (Roche). All hybridizations were performed using at least three biological replicates.

EMSA

EMSAs were performed according to a recent report (Wang et al., 2011). Briefly, the N terminus of RhNAC100 was fused in frame to GST and expressed in *Escherichia coli* BL21. The fused protein was induced by adding isopropylthio-β-galactoside (0.2 mM), and the cells were incubated at 170 rpm for 6 h at 28°C. The recombinant protein was purified using Glutathione Sepharose 4B (GE Healthcare) according to the manufacturer's instructions. EMSAs were performed using the LightShift chemiluminescent EMSA kit (Pierce) according to the manufacturer's instructions.

ChIP Assay

ChIP assays were performed using Arabidopsis protoplasts as described previously (Hao et al., 2012). The mesophyll protoplasts were isolated from Arabidopsis leaves (Col-0) transformed with *RhCesA2*, *RhPIP1;1*, or *RhPIP2;1* promoters. The plasmid *35S:RhNAC100-GFP* was transfected into the protoplasts. After transfection and incubation at room temperature overnight, the protoplasts were fixed for 20 min using formaldehyde (final concentration, 1% [v/v]). The chromatin complex was fragmented by sonication and incubated with anti-GFP antibody-Protein A beads overnight. After washing, the beads were incubated at 65°C for 6 h for reverse cross linking, and the coprecipitated DNA was purified. The DNA was analyzed using semiquantitative reverse transcription-PCR and quantitative real-time PCR using the Bioline SYBR master mix (Bio-Rad). Primers for the ChIP-PCR are listed in Supplemental Table S1.

The GenBank accession numbers of the sequences are as follows: *RhNAC100* (JQ001774), *RhCesA2* (JQ001775), *ATNAC2* (NP_198777), *ATNAC3* (NP_189546), *ANAC100* (NP_200951), *ANAC080* (NP_568182), *ANAC087* (NP_197328), *ANAC046* (NP_187056), *CUC2* (NP_200206), *CUC1* (NP_188135), *CUC3* (NP_177768), *NAC1* (NP_175997), and *ANAC074* (NP_567811).

Supplemental Data

The following materials are available in the online version of this article.

Supplemental Figure S1. Generation and assembly of high-quality sequences from rose flowers.

Supplemental Figure S2. Alignment and phylogenetic tree of RhNAC100 with known NAC-domain proteins, expression in different organs, and transcription activity assay of RhNAC100.

Supplemental Figure S3. qRT-PCR of RhNAC100 and rhy-miR164 in petals treated by NAA, GA, or brassinosteroid.

Supplemental Figure S4. Promoter analysis of RhNAC100 and region amplification-PCR of RhNAC100 during flower opening.

Supplemental Figure S5. Phenotype of transgenic Arabidopsis plants overexpressing RhNAC100 and RhNAC100m.

Supplemental Figure S6. qRT-PCR of five RhNAC100 homologous genes in RhNAC100-silenced petals.

Supplemental Figure S7. Functional characterization of a RhNAC100 downstream gene, RhCesA2, in rose petals.

Supplemental Table S1. Oligonucleotide primer sequences used in this work.

Supplemental Table S2. GO slim classification of rose assembled transcripts.

Supplemental Table S3. List of 2,189 ethylene-responsive assembled transcripts in rose petals.

Supplemental Table S4. List of ethylene-responsive TFs and TRs.

Supplemental Table S5. Changes in gene expression in transgenic Arabidopsis plants overexpressing RhNAC100m.

Supplemental Table S6. qRT-PCR of 29 putative downstream genes of RhNAC100 in petals during natural flower opening.

Supplemental Table S7. List of biochemical pathways altered in rose petals in response to ethylene.

Supplemental Table S8. List of cellulose synthase genes significantly down-regulated by ethylene in rose petals.

Supplemental Text S1. Supplemental Materials and Methods.

ACKNOWLEDGMENTS

We thank Shou-Yi Chen and Jin-Song Zhang (Chinese Academy of Sciences) for providing the *ein2-1* mutant and the vectors of transcription activity assay, Zhizhong Gong (China Agricultural University) for his generous help with the EMSA assays, Zhiyong Wang (Carnegie Institution for Science) for his generous help with the ChIP assays, Yule Liu (Tsinghua University) for his excellent advice, and Elizabeth Baldwin (U.S. Department of Agriculture-Agricultural Research Service, Citrus and Subtropical Products Laboratory) for proofreading our manuscript.

Received June 17, 2013; accepted August 8, 2013; published August 9, 2013.

LITERATURE CITED

Abeles FB, Morgan PW, Saltveit MEJ (1992) Ethylene in Plant Biology. Academic Press, Inc., San Diego

Achard P, Baghour M, Chapple A, Hedden P, Van Der Straeten D, Genschik P, Moritz T, Harberd NP (2007) The plant stress hormone ethylene controls floral transition via DELLA-dependent regulation of floral meristem-identity genes. Proc Natl Acad Sci USA **104:** 6484–6489

Achard P, Herr A, Baulcombe DC, Harberd NP (2004) Modulation of floral development by a gibberellin-regulated microRNA. Development **131:** 3357–3365

Achard P, Vriezen WH, Van Der Straeten D, Harberd NP (2003) Ethylene regulates *Arabidopsis* development via the modulation of DELLA protein growth repressor function. Plant Cell **15:** 2816–2825

Aida M, Ishida T, Fukaki H, Fujisawa H, Tasaka M (1997) Genes involved in organ separation in *Arabidopsis*: an analysis of the *cup-shaped cotyledon* mutant. Plant Cell **9:** 841–857

Aida M, Tasaka M (2006) Genetic control of shoot organ boundaries. Curr Opin Plant Biol **9:** 72–77

Alba R, Payton P, Fei Z, McQuinn R, Debbie P, Martin GB, Tanksley SD, Giovannoni JJ (2005) Transcriptome and selected metabolite analyses reveal multiple points of ethylene control during tomato fruit development. Plant Cell **17:** 2954–2965

Baker CC, Sieber P, Wellmer F, Meyerowitz EM (2005) The *early extra petals1* mutant uncovers a role for microRNA *miR164c* in regulating petal number in *Arabidopsis*. Curr Biol **15:** 303–315

Balazadeh S, Siddiqui H, Allu AD, Matallana-Ramirez LP, Caldana C, Mehrnia M, Zanor MI, Köhler B, Mueller-Roeber B (2010) A gene regulatory network controlled by the NAC transcription factor ANAC092/AtNAC2/ORE1 during salt-promoted senescence. Plant J **62:** 250–264

Bartel DP (2009) MicroRNAs: target recognition and regulatory functions. Cell **136:** 215–233

Bendahmane M, Dubois A, Raymond O, Bris ML (2013) Genetics and genomics of flower initiation and development in roses. J Exp Bot **64:** 847–857

Benjamini Y, Hochberg Y (1995) Controlling the false discovery rate: a practical and powerful approach to multiple testing. J R Stat Soc, B **57:** 289–300

Bolstad BM, Irizarry RA, Astrand M, Speed TP (2003) A comparison of normalization methods for high density oligonucleotide array data based on variance and bias. Bioinformatics **19:** 185–193

Channelière S, Rivière S, Scalliet G, Szecsi J, Jullien F, Dolle C, Vergne P, Dumas C, Bendahmane M, Hugueney P, et al (2002) Analysis of gene expression in rose petals using expressed sequence tags. FEBS Lett **515:** 35–38

Chen W, Yin X, Wang L, Tian J, Yang RY, Liu DF, Yu ZH, Ma N, Gao JP (2013) Involvement of rose aquaporin RhPIP1;1 in ethylene-regulated petal expansion through interaction with RhPIP2;1. Plant Mol Biol

Chu Z, Chen H, Zhang Y, Zhang Z, Zheng N, Yin B, Yan H, Zhu L, Zhao X, Yuan M, et al (2007) Knockout of the *AtCESA2* gene affects microtubule orientation and causes abnormal cell expansion in Arabidopsis. Plant Physiol **143:** 213–224

Cosgrove DJ (2005) Growth of the plant cell wall. Nat Rev Mol Cell Biol **6:** 850–861

de Hoon MJ, Imoto S, Nolan J, Miyano S (2004) Open source clustering software. Bioinformatics **20:** 1453–1454

De Paepe A, Vuylsteke M, Van Hummelen P, Zabeau M, Van Der Straeten D (2004) Transcriptional profiling by cDNA-AFLP and microarray analysis reveals novel insights into the early response to ethylene in *Arabidopsis*. Plant J **39:** 537–559

Dubois A, Carrere S, Raymond O, Pouvreau B, Cottret L, Roccia A, Onesto JP, Sakr S, Atanassova R, Baudino S, et al (2012) Transcriptome database resource and gene expression atlas for the rose. BMC Genomics **13:** 638

Dubois A, Remay A, Raymond O, Balzergue S, Chauvet A, Maene M, Pécrix Y, Yang SH, Jeauffre J, Thouroude T, et al (2011) Genomic approach to study floral development genes in *Rosa* spp. PLoS ONE **6:** e28455

Dunoyer P, Lecellier CH, Parizotto EA, Himber C, Voinnet O (2004) Probing the microRNA and small interfering RNA pathways with virus-encoded suppressors of RNA silencing. Plant Cell **16:** 1235–1250

Eisen MB, Spellman PT, Brown PO, Botstein D (1998) Cluster analysis and display of genome-wide expression patterns. Proc Natl Acad Sci USA **95:** 14863–14868

Guo HS, Xie Q, Fei JF, Chua NH (2005) MicroRNA directs mRNA cleavage of the transcription factor *NAC1* to downregulate auxin signals for *Arabidopsis* lateral root development. Plant Cell **17:** 1376–1386

Guterman I, Shalit M, Menda N, Piestun D, Dafny-Yelin M, Shalev G, Bar E, Davydov O, Ovadis M, Emanuel M, et al (2002) Rose scent: genomics approach to discovering novel floral fragrance-related genes. Plant Cell **14:** 2325–2338

Guzmán P, Ecker JR (1990) Exploiting the triple response of *Arabidopsis* to identify ethylene-related mutants. Plant Cell **2:** 513–523

Hao Y, Oh E, Choi G, Liang Z, Wang ZY (2012) Interactions between HLH and bHLH factors modulate light-regulated plant development. Mol Plant **5:** 688–697

Hao YJ, Song QX, Chen HW, Zou HF, Wei W, Kang XS, Ma B, Zhang WK, Zhang JS, Chen SY (2010) Plant NAC-type transcription factor proteins contain a NARD domain for repression of transcriptional activation. Planta **232:** 1033–1043

Hao YJ, Wei W, Song QX, Chen HW, Zhang YQ, Wang F, Zou HF, Lei G, Tian AG, Zhang WK, et al (2011) Soybean NAC transcription factors promote abiotic stress tolerance and lateral root formation in transgenic plants. Plant J **68:** 302–313

Hasson A, Plessis A, Blein T, Adroher B, Grigg S, Tsiantis M, Boudaoud A, Damerval C, Laufs P (2011) Evolution and diverse roles of the *CUP-SHAPED COTYLEDON* genes in *Arabidopsis* leaf development. Plant Cell **23:** 54–68

He XJ, Mu RL, Cao WH, Zhang ZG, Zhang JS, Chen SY (2005) AtNAC2, a transcription factor downstream of ethylene and auxin signaling pathways, is involved in salt stress response and lateral root development. Plant J **44:** 903–916

Hu R, Qi G, Kong Y, Kong D, Gao Q, Zhou GK (2010) Comprehensive analysis of NAC domain transcription factor gene family in *Populus trichocarpa*. BMC Plant Biol **10:** 145

Irish VF (2008) The *Arabidopsis* petal: a model for plant organogenesis. Trends Plant Sci **13:** 430–436

Jaillais Y, Chory J (2010) Unraveling the paradoxes of plant hormone signaling integration. Nat Struct Mol Biol **17:** 642–645

Jensen MK, Kjaersgaard T, Petersen K, Skriver K (2010) NAC genes: time-specific regulators of hormonal signaling in Arabidopsis. Plant Signal Behav **5:** 907–910

Jia HF, Chai YM, Li CL, Lu D, Luo JJ, Qin L, Shen YY (2011) Abscisic acid plays an important role in the regulation of strawberry fruit ripening. Plant Physiol **157:** 188–199

Jones-Rhoades MW, Bartel DP (2004) Computational identification of plant microRNAs and their targets, including a stress-induced miRNA. Mol Cell **14:** 787–799

Joung JG, Corbett AM, Fellman SM, Tieman DM, Klee HJ, Giovannoni JJ, Fei Z (2009) Plant MetGenMAP: an integrative analysis system for plant systems biology. Plant Physiol **151:** 1758–1768

Khraiwesh B, Zhu JK, Zhu J (2012) Role of miRNAs and siRNAs in biotic and abiotic stress responses of plants. Biochim Biophys Acta **1819:** 137–148

Kieber JJ, Rothenberg M, Roman G, Feldmann KA, Ecker JR (1993) *CTR1*, a negative regulator of the ethylene response pathway in *Arabidopsis*, encodes a member of the raf family of protein kinases. Cell **72:** 427–441

Kim J, Park JH, Lim CJ, Lim JY, Ryu JY, Lee BW, Choi JP, Kim WB, Lee HY, Choi Y, et al (2012) Small RNA and transcriptome deep sequencing proffers insight into floral gene regulation in *Rosa* cultivars. BMC Genomics **13:** 657

Kim JH, Woo HR, Kim J, Lim PO, Lee IC, Choi SH, Hwang D, Nam HG (2009) Trifurcate feed-forward regulation of age-dependent cell death involving *miR164* in *Arabidopsis*. Science **323:** 1053–1057

Ko JH, Yang SH, Park AH, Lerouxel O, Han KH (2007) ANAC012, a member of the plant-specific NAC transcription factor family, negatively regulates xylary fiber development in *Arabidopsis thaliana*. Plant J **50:** 1035–1048

Koyama T, Furutani M, Tasaka M, Ohme-Takagi M (2007) TCP transcription factors control the morphology of shoot lateral organs via negative regulation of the expression of boundary-specific genes in *Arabidopsis*. Plant Cell **19:** 473–484

Larue CT, Wen J, Walker JC (2009) Genetic interactions between the *miRNA164-CUC2* regulatory module and *BREVIPEDICELLUS* in *Arabidopsis* developmental patterning. Plant Signal Behav **4:** 666–668

Laufs P, Peaucelle A, Morin H, Traas J (2004) MicroRNA regulation of the CUC genes is required for boundary size control in *Arabidopsis* meristems. Development **131:** 4311–4322

Llave C, Xie Z, Kasschau KD, Carrington JC (2002) Cleavage of *Scarecrow*-like mRNA targets directed by a class of *Arabidopsis* miRNA. Science **297:** 2053–2056

Love J, Björklund S, Vahala J, Hertzberg M, Kangasjärvi J, Sundberg B (2009) Ethylene is an endogenous stimulator of cell division in the cambial meristem of *Populus*. Proc Natl Acad Sci USA **106:** 5984–5989

Ma N, Cai L, Lu WJ, Tan H, Gao JP (2005) Exogenous ethylene influences flower opening of cut roses (*Rosa hybrida*) by regulating the genes encoding ethylene biosynthesis enzymes. Sci China C Life Sci **48:** 434–444

Ma N, Tan H, Liu X, Xue J, Li Y, Gao J (2006) Transcriptional regulation of ethylene receptor and *CTR* genes involved in ethylene-induced flower opening in cut rose (*Rosa hybrida*) cv. Samantha. J Exp Bot **57:** 2763–2773

Ma N, Xue J, Li Y, Liu X, Dai F, Jia W, Luo Y, Gao J (2008) *Rh-PIP2;1*, a rose aquaporin gene, is involved in ethylene-regulated petal expansion. Plant Physiol **148:** 894–907

Mallory AC, Dugas DV, Bartel DP, Bartel B (2004) MicroRNA regulation of NAC-domain targets is required for proper formation and separation of adjacent embryonic, vegetative, and floral organs. Curr Biol **14:** 1035–1046

Mitsuda N, Seki M, Shinozaki K, Ohme-Takagi M (2005) The NAC transcription factors NST1 and NST2 of *Arabidopsis* regulate secondary wall thickenings and are required for anther dehiscence. Plant Cell **17:** 2993–3006

Mizukami Y, Fischer RL (2000) Plant organ size control: *AINTEGUMENTA* regulates growth and cell numbers during organogenesis. Proc Natl Acad Sci USA **97:** 942–947

Muday GK, Rahman A, Binder BM (2012) Auxin and ethylene: collaborators or competitors? Trends Plant Sci **17:** 181–195

Nikovics K, Blein T, Peaucelle A, Ishida T, Morin H, Aida M, Laufs P (2006) The balance between the *MIR164A* and *CUC2* genes controls leaf margin serration in *Arabidopsis*. Plant Cell **18:** 2929–2945

Oh TJ, Wartell RM, Cairney J, Pullman GS (2008) Evidence for stage-specific modulation of specific microRNAs (miRNAs) and miRNA processing components in zygotic embryo and female gametophyte of loblolly pine (*Pinus taeda*). New Phytol **179:** 67–80

Olsen AN, Ernst HA, Leggio LL, Skriver K (2005) NAC transcription factors: structurally distinct, functionally diverse. Trends Plant Sci **10:** 79–87

Ortega-Martinez O, Pernas M, Carol RJ, Dolan L (2007) Ethylene modulates stem cell division in the *Arabidopsis thaliana* root. Science **317:** 507–510

Peaucelle A, Morin H, Traas J, Laufs P (2007) Plants expressing a *miR164*-resistant *CUC2* gene reveal the importance of post-meristematic maintenance of phyllotaxy in *Arabidopsis*. Development **134:** 1045–1050

Pierik R, Tholen D, Poorter H, Visser EJ, Voesenek LA (2006) The Janus face of ethylene: growth inhibition and stimulation. Trends Plant Sci **11:** 176–183

Pinheiro GL, Marques CS, Costa MD, Reis PA, Alves MS, Carvalho CM, Fietto LG, Fontes EP (2009) Complete inventory of soybean NAC transcription factors: sequence conservation and expression analysis uncover their distinct roles in stress response. Gene **444:** 10–23

Raman S, Greb T, Peaucelle A, Blein T, Laufs P, Theres K (2008) Interplay of miR164, *CUP-SHAPED COTYLEDON* genes and *LATERAL SUPPRESSOR* controls axillary meristem formation in *Arabidopsis thaliana*. Plant J **55:** 65–76

Rhoades MW, Reinhart BJ, Lim LP, Burge CB, Bartel B, Bartel DP (2002) Prediction of plant microRNA targets. Cell **110:** 513–520

Riechmann JL, Heard J, Martin G, Reuber L, Jiang C, Keddie J, Adam L, Pineda O, Ratcliffe OJ, Samaha RR, et al (2000) *Arabidopsis* transcription factors: genome-wide comparative analysis among eukaryotes. Science **290:** 2105–2110

Romualdi C, Bortoluzzi S, D'Alessi F, Danieli GA (2003) IDEG6: a web tool for detection of differentially expressed genes in multiple tag sampling experiments. Physiol Genomics **12:** 159–162

Rushton PJ, Bokowiec MT, Laudeman TW, Brannock JF, Chen X, Timko MP (2008) TOBFAC: the database of tobacco transcription factors. BMC Bioinformatics **9:** 53

Růzicka K, Ljung K, Vanneste S, Podhorská R, Beeckman T, Friml J, Benková E (2007) Ethylene regulates root growth through effects on auxin biosynthesis and transport-dependent auxin distribution. Plant Cell **19:** 2197–2212

Sieber P, Wellmer F, Gheyselinck J, Riechmann JL, Meyerowitz EM (2007) Redundancy and specialization among plant microRNAs: role of the *MIR164* family in developmental robustness. Development **134:** 1051–1060

Sisler EC, Serek M (1997) Inhibitors of ethylene responses in plants at the receptor level: recent developments. Physiol Plant **100:** 577–582

Souret FF, Kastenmayer JP, Green PJ (2004) AtXRN4 degrades mRNA in *Arabidopsis* and its substrates include selected miRNA targets. Mol Cell **15:** 173–183

Spitzer-Rimon B, Marhevka E, Barkai O, Marton I, Edelbaum O, Masci T, Prathapani NK, Shklarman E, Ovadis M, Vainstein A (2010) *EOBII*, a gene encoding a flower-specific regulator of phenylpropanoid volatiles' biosynthesis in petunia. Plant Cell **22:** 1961–1976

Stepanova AN, Robertson-Hoyt J, Yun J, Benavente LM, Xie DY, Dolezal K, Schlereth A, Jürgens G, Alonso JM (2008) *TAA1*-mediated auxin biosynthesis is essential for hormone crosstalk and plant development. Cell **133:** 177–191

Stepanova AN, Yun J, Likhacheva AV, Alonso JM (2007) Multilevel interactions between ethylene and auxin in *Arabidopsis* roots. Plant Cell **19:** 2169–2185

Sunkar R, Zhu JK (2004) Novel and stress-regulated microRNAs and other small RNAs from *Arabidopsis*. Plant Cell **16:** 2001–2019

Swarup R, Perry P, Hagenbeek D, Van Der Straeten D, Beemster GT, Sandberg G, Bhalerao R, Ljung K, Bennett MJ (2007) Ethylene upregulates auxin biosynthesis in *Arabidopsis* seedlings to enhance inhibition of root cell elongation. Plant Cell **19:** 2186–2196

Tan H, Liu X, Ma N, Xue J, Lu W, Bai J, Gao J (2006) Ethylene-influenced flower opening and expression of genes encoding *Etrs*, *Ctrs*, and *Ein3s* in two cut rose cultivars. Postharvest Biol Technol **40:** 97–105

Taylor NG (2008) Cellulose biosynthesis and deposition in higher plants. New Phytol **178:** 239–252

Tran LS, Nakashima K, Sakuma Y, Simpson SD, Fujita Y, Maruyama K, Fujita M, Seki M, Shinozaki K, Yamaguchi-Shinozaki K (2004) Isolation and functional analysis of *Arabidopsis* stress-inducible NAC transcription factors that bind to a drought-responsive *cis*-element in the *early responsive to dehydration stress 1* promoter. Plant Cell **16:** 2481–2498

Vandenbussche F, Vancompernolle B, Rieu I, Ahmad M, Phillips A, Moritz T, Hedden P, Van Der Straeten D (2007) Ethylene-induced *Arabidopsis* hypocotyl elongation is dependent on but not mediated by gibberellins. J Exp Bot **58:** 4269–4281

Varaud E, Brioudes F, Szécsi J, Leroux J, Brown S, Perrot-Rechenmann C, Bendahmane M (2011) AUXIN RESPONSE FACTOR8 regulates *Arabidopsis* petal growth by interacting with the bHLH transcription factor BIGPETALp. Plant Cell **23:** 973–983

Vazquez F, Gasciolli V, Crété P, Vaucheret H (2004) The nuclear dsRNA binding protein HYL1 is required for microRNA accumulation and plant development, but not posttranscriptional transgene silencing. Curr Biol **14:** 346–351

Vriezen WH, Achard P, Harberd NP, Van Der Straeten D (2004) Ethylene-mediated enhancement of apical hook formation in etiolated *Arabidopsis thaliana* seedlings is gibberellin dependent. Plant J **37:** 505–516

Wang L, Hua D, He J, Duan Y, Chen Z, Hong X, Gong Z (2011) *Auxin Response Factor2* (*ARF2*) and its regulated homeodomain gene *HB33* mediate abscisic acid response in *Arabidopsis*. PLoS Genet **7:** e1002172

Weiss D, Ori N (2007) Mechanisms of cross talk between gibberellin and other hormones. Plant Physiol **144:** 1240–1246

Xiong Y, Liu T, Tian C, Sun S, Li J, Chen M (2005) Transcription factors in rice: a genome-wide comparative analysis between monocots and eudicots. Plant Mol Biol **59:** 191–203

Xue J, Yang F, Gao J (2009) Isolation of *Rh-TIP1;1*, an aquaporin gene and its expression in rose flowers in response to ethylene and water deficit. Postharvest Biol Technol **51:** 407–413

Yamada K, Norikoshi R, Suzuki K, Nishijima T, Imanishi H, Ichimura K (2009) Cell division and expansion growth during rose petal development. J Jpn Soc Hortic Sci **78:** 356–362

Yamaguchi M, Demura T (2010) Transcriptional regulation of secondary wall formation controlled by NAC domain proteins. Plant Biotechnol **27:** 237–242

Yamaguchi M, Mitsuda N, Ohtani M, Ohme-Takagi M, Kato K, Demura T (2011) VASCULAR-RELATED NAC-DOMAIN7 directly regulates the expression of a broad range of genes for xylem vessel formation. Plant J **66:** 579–590

Yoo SD, Cho Y, Sheen J (2009) Emerging connections in the ethylene signaling network. Trends Plant Sci **14:** 270–279

Zhong GY, Burns JK (2003) Profiling ethylene-regulated gene expression in *Arabidopsis thaliana* by microarray analysis. Plant Mol Biol **53:** 117–131

Zhong R, Demura T, Ye ZH (2006) SND1, a NAC domain transcription factor, is a key regulator of secondary wall synthesis in fibers of *Arabidopsis*. Plant Cell **18:** 3158–3170

Zhong R, Lee C, Ye ZH (2010) Functional characterization of poplar wood-associated NAC domain transcription factors. Plant Physiol **152:** 1044–1055